THE DEVELOPMENT OF A PAN-CENTROMERIC MARKER TO QUANTIFY CELLULAR RADIATION DAMAGE IN HEALTHY INDIVIDUALS AND IN AN HIV COHORT

Rosemary Veronica Swanson, 0402274D

A dissertation submitted to the Faculty of Health Sciences, University of the Witwatersrand, Johannesburg, in fulfilment of the requirements for the degree of Master of Science.

Johannesburg, 2010

Declaration

I declare that this dissertation is my own unaided work. It is being submitted for the degree of Master of Science to the University of the Witwatersrand, Johannesburg. It has not been submitted before for any degree or examination in any other University.

_____

(Signature of candidate)

_____ day of _____ 2010.

Abstract

INTRODUCTION: Ionising radiation can induce DNA damage, in the form of DNA double strand breaks (DSBs), which the affected cell may or may not be able to repair. Micronuclei are indicators of cytogenetic damage, which result from aneugenic (spontaneous loss of chromosomes) or clastogenic (chromosomal fragments) events. The micronuclei may be centromere-positive (CM+MN) for aneugenic events or centromere-negative (CM–MN) for clastogenic events. A pan-centromeric marker would help differentiate between CM+MN and CM–MN, especially important among exposures to very low doses of ionising radiation.

METHODOLOGY: Micronucleus assays were performed on blood samples collected from healthy donors and HIV+ donors. The blood samples were irradiated at various doses of ionising radiation. Two methods were used to create a pan-centromeric probe. First, the p82H plasmid, which contains centromere specific α repetitive human DNA sequences, was used. Second, human centromeric sequences were amplified using polymerase chain reaction (PCR). In both cases, the pan-centromeric probe was labelled and hybridised using fluorescent *in situ* hybridisation (FISH) to micronucleus slide preparations from healthy and HIV+ donors. The slides were scored manually and on an automated system, MetaFer®.

RESULTS: The p82H probe did not hybridise to any centromeres when FISH was performed, while the synthetic probe made by means of PCR bound to the centromeres of all chromosomes. Henceforth, all experiments were performed with the synthetic pan-centromeric probe. A dose response study was performed on micronucleus slides from healthy donors, from which significant differences in the number of micronuclei and the percentage of centromere-negative micronuclei could be seen between doses. The HIV study involving HIV+ donors and HIV– controls did not yield any significant differences between the two groups.

DISCUSSION & CONCLUSION: Combining the micronucleus assay with the pan-centromeric probe greatly improves its sensitivity. The dose response study corroborated previous work performed by Vral et al (1997). Contrary to what was expected and published (Baeyens et al, 2010), no significant differences were observed between HIV+ and HIV- individuals. Issues, improvements and possible future work are discussed.

Acknowledgments

I would like to acknowledge and thank iThemba LABS and the Flemish InterUniversity Council (VLIR) for funding this project.

My thanks to the Department of Basic Medical Science, University of Ghent, and the Institute for Nuclear Sciences (INW) in Belgium for the use of their facilities and the support of their expertise in performing the relevant radiations and assays, and for the opportunity of collaborating with them in this research.

I would like to thanks Medical Physics, Charlotte Maxeke Hospital, South Africa for granting the use of their facilities and their expertise performing the radiations on the premises.

I would also like to express my appreciation to the Somatic Cell Genetics Unit, Department of Molecular Medicine and Haematology, University of the Witwatersrand, South Africa for any and all help with regards to this project in using their equipment and laboratory, and for teaching me many of the techniques utilised in this study.

I would especially like to thank my supervisors Ans Baeyens and Pascale Willem for their guidance and encouragement throughout the project.

Table of Contents

List of Figures

List of tables

List of symbols

°C	degrees celsius
%	percentage
×	multiplication
×g	g-force
∞	infinity → indicates that reaction can be held/stored at this temperature
3'-	end of DNA strand; named according to the number of carbon atoms in the deoxyribose sugar
5'-	end of DNA strand; named according to the number of carbon atoms in the deoxyribose sugar; will connect to 3'-end of another strand
bp	base pairs
cells/mm^3	number of cells per cubic millimetre
cm	centimetres
cm^3	cubic centimetres
Gy	Gray (unit of measurement for absorbed dose in radiation)
Gy/min	Gray per minute; dose rate
kb	kilobases
kDa	kilo Daltons
l	litre
µg	micrograms
µg/ml	micrograms per millilitre
µl	microlitre
µm^2	square micrometres
µM	micromolar
mg	milligrams
mg/ml	milligram per millilitre

ml	millilitre
mM	millimolar
M	molar
N	normal
ng	nanogram
ng/µl	nanograms per microlitre
nm	nanometres
rpm	revolutions per minute
U	unit
U/l	units per litre

Nomenclature

8-oxoG	8-oxoguanine
AALD	Activation-Associated Lymphocyte Death
AIDS	Acquired ImmunoDeficiency Syndrome
ALARA	As Low As Reasonably Possible
ARV	antiretroviral
ATM	Ataxia telangiectasia gene mutated
ATR	Ataxia telangiectasia related
AZT	3-azido-3-deoxythymidine
BAC	Bacterial Artificial Chromosome
BASC	BRCA1-associated surveillence complex
BER	base excision repair
BN	binucleated
BRCA1	Breast Cancer gene 1
C+MN	centromere positive micronucleus / micronuclei
C–MN	centromere negative micronucleus / micronuclei
CBMN assay	cytokinesis blocked micronucleus assay
CCR5	chemokine (C-C motif) receptor 5, glycoprotein, co-receptor (of HIV-1) on the surface of T-cells
CD4	Cluster of differentiation 4, glycoprotein, receptor (of HIV-1) on the surface of T-cells
CD8	Cluster of differentiation 8
CD4+	T-cells that have the CD4 receptor
CD8+	T-cells that have a CD8 receptor
Co-60	cobalt-60
CXCR4	CXC chemokine receptor, co-receptor (of HIV-1) on the surface of T-cells
Cyto B	cytochalasin B
DAPI	4', 6-diamidino-2-phenylindole

DOP-PCR	Degenerative Oligonucleotide Primed-PCR
DNA	deoxyribose nucleic acid
DSB	double strand breaks
EDTA	ethylenediaminetetraacetic acid
FCS	foetal calf serum
FISH	Fluorescent *in situ* hybridisation
Gag	group-specific antigen
gp41	41 kDa transmembrane glycoprotein
gp120	120 kDa docking glycoprotein
HAART	Highly Active AntiRetroviral Treatment
HCl	hydrogen chloride
HIV	human immunodeficiency virus
HIV+	HIV positive (infected)
HIV–	HIV negative (uninfected)
HR	homologous recombination
KCl	potassium chloride
LB	luria broth
LET	linear energy transfer
Li-heparin	lithium heparin
LNT	linear no threshold
$MgCl_2$	magnesium chloride
MMR	mismatch repair
MN	micronucleus / micronuclei
NER	nucleotide excision repair
NHEJ	non-homologous end-joining
p24	24 kDa capsid protein
PBS	phosphate buffered saline
PCR	polymerase chain reaction
PFA	paraformaldehyde
PHA	phytohaemagglutinin

PIC	pro-integration complex
Rev	regulator of virion
RNA	ribonucleic acid
R.o.I.	Region of interest
SCGE assay	Single Cell Gel Electrophoresis (Comet assay)
SDS	sodium dodecyl sulphate
SSB	single strand breaks
SSC	sodium saline citrate
TAE	Tris base, acetic acid, EDTA
TAR	transactivation response element
Tat	trans-activator of transcription
TBE	Tris base, boric acid, EDTA
TE	Tris EDTA
Tris	tris(hydroxymethyl)aminomethane
Vpr	Viral Protein R

CHAPTER ONE: INTRODUCTION

1.1 Radiobiology

Radiobiology is the study of what happens after an organism absorbs energy from ionising radiation, what it does to compensate for the effects of this energy and what types of damage are caused.

1.1.1 Ionising Radiation

Radiation is defined as energy that is travelling in waves or high-speed particles. Ionising radiation has enough energy to separate at least one electron from a molecule. The various types of ionising radiation can be divided into high- and low-LET (linear energy transfer) radiation. The LET of the radiation determines how effective a dose of radiation is in generating residual (unrepaired) cellular damage. High-LET radiation like neutrons and alpha-particles induce much more cellular damage per unit of radiation energy absorbed compared with that from low-LET sources of radiation e.g. gamma rays and X-rays. Ionising radiation can be produced by radioactive decay, nuclear fission, nuclear fusion, and particle accelerators (Dianiak et al, 2003; Tubiana et al, 1990). Gamma and X-radiation have different origins – gamma radiation originates from processes inside the nucleus, while X-radiation from processes outside the nucleus, such as a change in electron structure of an atom, and is mostly electronically produced.

Ionising radiation causes damage in living tissues by producing ionisations upon interaction with a cell. These ionisations can disrupt molecules, such as DNA, directly and/or indirectly by producing highly reactive free radicals, which will lead to DNA damage. Ionising radiation can have a variety of biological effects, such as damaging the integrity of the cell leading to cell death, disrupting protein molecules, causing lesions in sugars, as well as inducing DNA damage, which can result in changes in gene

expression, gene mutations, chromosomal aberrations, and genomic instability. A sufficient number of genetic alterations, may eventually lead to the development of cancer. Because ionising radiation is very effective in generating cellular damage and killing cells, it is used in the treatment of cancer. Ionising radiation is used in many disciplines from medicine to industrial applications. The dangers associated with radiation exposure depend on the strength of radiation, the type of radiation and length of exposure. The damage caused by radiation is divided into early effects, which occur shortly after exposure, but usually only with high doses i.e. acute exposure, and late effects, which happen years after exposure, and even at low doses i.e. chronic exposure (exposure to low doses may occur frequently over a long period) (Dianiak et al, 2003; Tubiana et al, 1990).

1.1.2 DNA damage and repair

Ionising radiation can have various effects on DNA and chromosomes. These include 1) changes to or loss of a base, 2) single strand breaks (SSB), where a lesion occurs in one strand of a DNA molecule, 3) double-strand breaks (DSB), in which breaks occur in both strands of a DNA molecule, 4) cross-linking within a DNA molecule (intrastrand) or between other DNA molecules (DNA interstrand) or other molecules (DNA-protein) and 5) the destruction of sugars. These different types of damage can occur separately, as simple lesions, which are mostly efficiently repaired, or they can occur together resulting in complex lesions, which are more difficult to repair, and are often repaired incorrectly or not at all. The un- or mis-repaired DSB often results in the formation of chromosomal aberrations (Tubiana et al, 1990).

The cell has various distinct repair mechanisms, which are activated in response to DNA damage along with cell cycle checkpoints. The type of

DNA damage determines what repair mechanism is to be used. There are five main DNA damage repair pathways in mammalian cells:

1) MisMatch Repair (MMR), which proofreads newly-synthesised DNA strands and fixes any mismatched bases that occur during replication and/or recombination,
2) Base Excision Repair (BER), which repairs small lesions, such as damaged bases, throughout the cell cycle,
3) Nucleotide Excision Repair (NER), which removes bulky lesions that distort the helix, and then DNA polymerase fills in the resulting gap,
4) Homologous Recombination (HR), which is responsible, along with
5) Non-Homologous End-Joining (NHEJ) for the repair of DNA DSBs (Christmann et al, 2003; Hoeijmakers, 2001).

The DSB is the most genotoxic DNA lesion induced by ionising radiation. A single DSB that remains unrepaired is capable of effecting apoptosis, or can induce other genotoxic effects, such as chromosomal breaks, loss and translocations (Christmann et al, 2003). The two main repair pathways of DNA DSBs, HR and NHEJ, are presented in Figure 1. The determination of which pathway is used to repair the DSB is dependent upon the phase of the cell cycle during which the DSB is detected in the cell. HR occurs mainly in late S and G2 phases, where homologous chromosomes are available, whilst NHEJ occurs in the G0/G1 phases of the cell cycle. In human cells, the majority of the DSBs are repaired by means of NHEJ, with only approximately 10% being repaired by means of HR (Christmann et al, 2003).

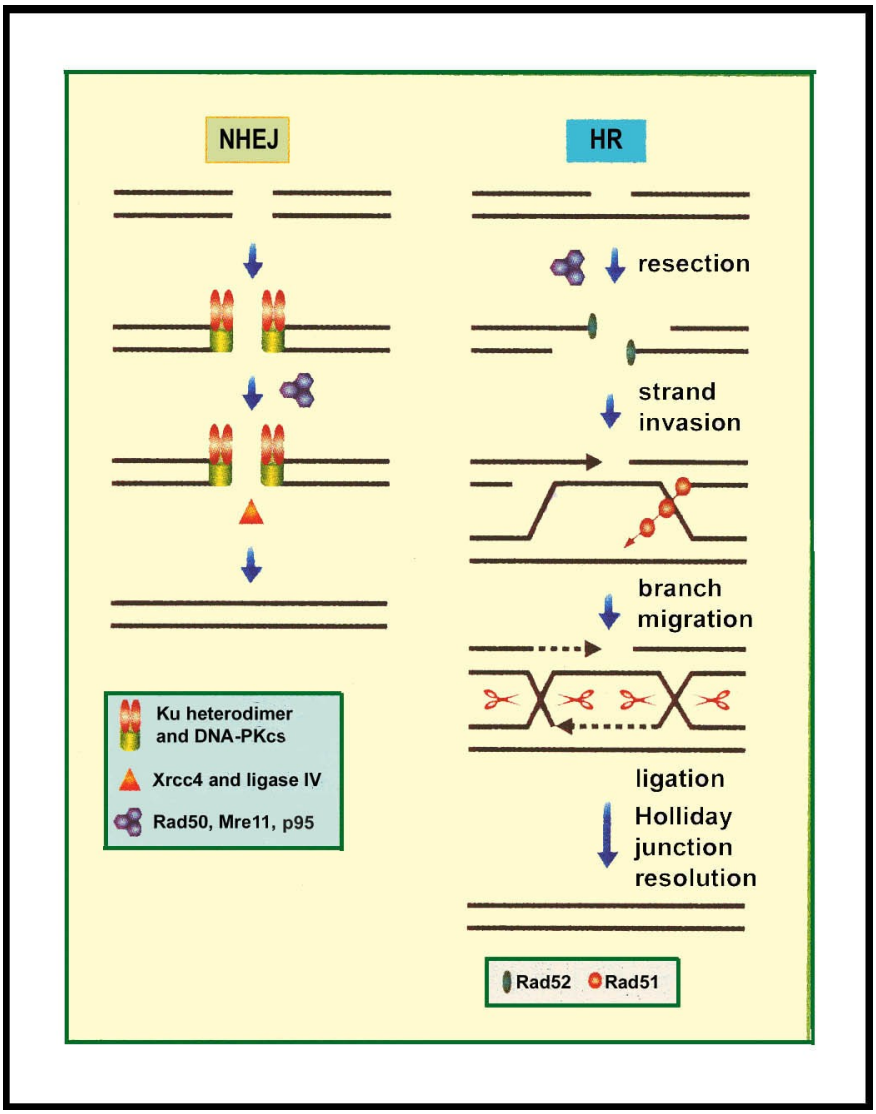

Figure 1: Representation of non-homologous end-joining (NHEJ) and homologous recombination (Khanna et al, 2001; modified)

HR is considered to be error-free as it involves copying information from undamaged chromosomes or chromatids to repair double strand breaks. It takes place more commonly in simple eukaryotes. The *RAD52* epistasis group, including genes such as *RAD51*, *RAD52* and *RAD54*, mediates the HR process (Kanaar et al., 1998; Pfeiffer et al., 2004). During HR, a DSB is cut from the 5'-end to the 3'-end by the MRE11-RAD50-NBS1 protein

complex. A complex made up of RAD52 proteins attaches itself to the 3' single stranded DNA, to protect it from exonucleolytic digestion. It has also been suggested that as RAD52 competes with the Ku protein to bind the DNA, it may influence the decision toward HR versus NHEJ. The RAD52 proteins interact with RAD51 and RPA proteins, which will effect RAD51's DNA exchange activity. Strand exchange events occur when the damaged strand interacts with homologous regions on an undamaged chromosome, displacing a strand from that chromosome; this is catalysed by the RAD51 protein. The RPA protein binds to the displaced strand thereby stabilising the pairing of the damaged and undamaged strands (Figure 1). A RAD51 nucleoprotein filament assembles, aided by the RAD51B, RAD51C, RAD51D, XRCRR2 and XRCRR3 proteins. HR then resolves, according to the Holliday model (Christmann et al, 2003).

NHEJ is the main mechanism by which irradiation-induced DSBs are removed in higher eukaryotes and it is regarded as being error-prone. NHEJ joins two ends of DSB without the requirement of sequence homology between the DNA ends. A heterodimer of Ku70 and Ku80 proteins bind to the DSB and protects the DNA from exonuclease digestion. The Ku heterodimer interacts with DNA-PK_{CS} and XRCC7 proteins to form the active DNA-PK holoenzyme. Thereafter, the MRE11-RAD50-NBS1 protein complex, which has exonuclease, endonuclease and helicase activity, processes DSBs by removing the 3'-flaps while the protein, FEN1 (flap endonuclease 1), removes the 5'-flaps. The protein, Artemis, forms a complex with DNA-PK_{CS} and aids in processing the 3'- and 5'-ends (Ma et al, 2002). The XRCC4 protein (a target of DNA-PK_{CS}) forms a stable complex with DNA ligase IV, which binds the ends of DNA molecules and joins them together (Christmann et al, 2003).

There are a variety of proteins involved in recognising and signalling DNA

damage, and checkpoint control. The phosphatidylinositol-3-kinases, such as ATM (Ataxia telangiectasia mutated), ATR (Ataxia telangiectasia related) and DNA-PK_{CS}, all recognise DNA breaks. ATM and ATR bind onto the ends of damaged DNA and activate their own kinase activity. Changes in chromatin structure, resulting from exposure to ionising radiation, may play a role in activating ATM. The DNA-damage repair proteins have also been found to be associated with surveillance complexes such as BASC (BRCA1-associated surveillence complex). BASC has been found to be associated with the following proteins, BRCA1, MSH2, MSH6, MLH1, ATM, BLM, and the MRE11-RAD50-NBS1 complex. The proteins, CHK1, CHK2 and p53, which are phosphorylated by ATM and/or ATR are important in signalling cell cycle arrest at G1/S and G2/M, as well as apoptosis; they also enhance DNA repair (Christmann et al, 2003).

It has been assumed that DNA repair responses occur equally efficiently at high and low doses of ionising radiation. However, Rothkamm and Lobrich (2003) found this was not the case in their study. Rather, they observed that at low doses, DSBs remain unrepaired, and if the cells were allowed to proliferate damaged cells are eliminated rather than being repaired.

1.1.3 Chromosomal aberrations

DNA DSBs are one of the major effects of ionising radiation. Chromosomal aberrations form when the DNA DSB is not repaired or mis-repaired. There are different types of chromosome aberrations that can be induced by ionising radiation, such as (Figure 2):

- acentric fragments,
- dicentrics,
- rings,

- translocations,
- inversions and
- deletions.

Chromatid aberrations may also occur and they include breaks or exchanges (Figure 2).

These chromosomal aberrations can be stable or unstable. Stable aberrations, such as translocations and inversions, occur because of symmetrical exchanges, and no genetic information is lost. Translocations can occur on the same chromosome, or between different chromosomes. Stable aberrations can result in altered gene expression, up-regulation of oncogenes and down-regulation of tumour suppressor genes, which may ultimately advance the development of cancer (Baeyens, 2005). Unstable aberrations, resulting from asymmetric exchanges, are those where genetic information is lost. One example is when acentric fragments, chromosomal fragments lacking a centromere, are expelled from the nucleus because they are unable to attach to the spindle apparatus during cell division. Nuclear membranes can form around these fragments to form micronuclei, which appear in the cytoplasm. As the nuclei lose this genetic information, the cell may stall in the cell cycle, and cell death may occur. Other examples of unstable aberrations include dicentric chromosomes and ring chromosomes (Tubiana et al, 1990).

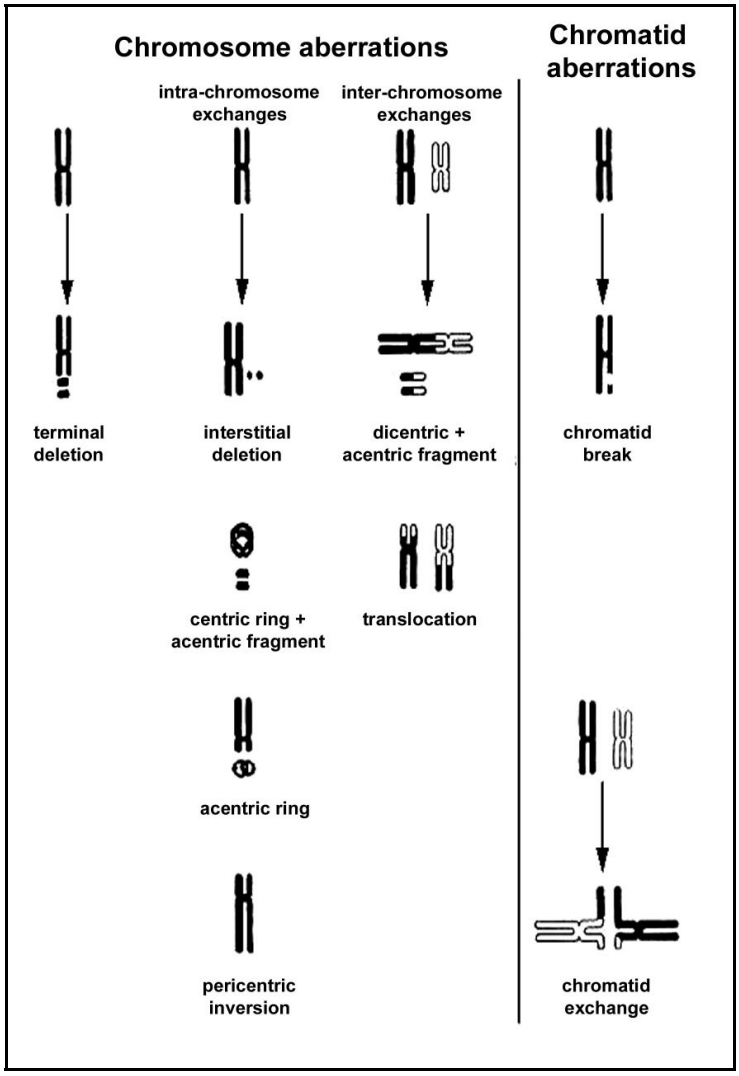

Figure 2: Different types of chromosome and chromatid aberrations (Tubiana et al., 1990)

1.1.4 Biodosimetry

Radiation protection legislation sets effective dose limits for occupational yearly exposure, which includes the sum of internal and external exposure, but not natural background radiation or medical exposure. The dose limits are often based on a linear-no-threshold (LNT) model, which assumes a worst case scenario; this often leads to an overestimation of the risks

involved.

When using ionising radiation, the following principles should be considered:

A) Justification Principle

The benefits of using ionising radiation must outweigh the risks involved, and its use must be justified when comparing it to the use of other techniques.

B) Optimisation

Exposure must be kept as low as reasonably achievable (ALARA).

C) Principle of Individual Dose Limits

Dose limits must never be surpassed. For every act involving radiation a study should be done to determine the lowest possible dose and risk to determine a working level of radiation exposure.

1.1.5 Biomonitoring

Human Bio Monitoring was defined by Zielhuis (1984) as " a systematic continuous or repetitive activity for collection of pollutants, metabolites or specific non-adverse biological effect parameters for immediate application, with the objective to assess exposure and health risk to exposed subjects, comparing the data observed with the reference level and – if necessary – leading to corrective actions."

Basically, biomonitoring refers to the use of scientific techniques to assess exposures to natural or synthetic agents or chemicals. Biomonitoring can be performed because chemicals and agents leave evidence in exposed individuals such as chemicals or their metabolites, or cellular components

that have been affected by exposure, such as ionising radiation. Tissues and/or fluids from exposed individuals are analysed to detect these "markers". Biomonitoring is categorised into 1) dose monitoring (defined as the determination of hazardous substances or their metabolites in body fluids), 2) biochemical effect monitoring (the quantification of the reaction products of reactive substances with biological molecules e.g. DNA or protein adducts) and 3) biological effect monitoring (the measurement of early biological effects caused by agents e.g micronuclei) (Angerer et al, 2007).

Angerer et al (2007) suggest several factors that should be fulfilled to ensure that the biomonitoring is suitable and dependable. Firstly, an appropriate biological matrix is required. The biological matrix needs to be easily obtainable from the patient, without causing harm to that person, but in adequate amounts to perform the tests required. Blood and urine are excellent examples fulfilling these criteria. Secondly, suitable parameters that reflect internal exposure, biochemical or biological effects are needed. Each biomarker has individual characteristics regarding sensitivity and specificity, and its usefulness can be influenced by the selection of biological specimens (Au, 2007). Micronuclei as well as other chromosomal aberrations are examples of early biological effect biomarkers. Thirdly, the analytical methods used need to be suitable for what is being looked for and on what specimen. The analytical methods also need to be reliable and reproducible. Finally, reference and limit values are needed. Reference values are statistical descriptions of the background exposure of a certain population group; limit values refer to the limits below which and above which harmless effects or harmful effects occur respectively (Angerer et al, 2007).

Dose response studies can be performed to establish reference values as well

as to determine “safe” and “hazardous” limit values. Dose response studies trace how an effect on an organism, caused by a stressor (such as ionising radiation) changes with respect to differing doses or levels of exposure after a certain time period. It is important to establish reference values in order to interpret results, and to establish individual reference values since there is individual variation regarding the expression of biomarkers – some are less susceptible while others are more susceptible to radiation (Au, 2007).

Biomonitoring is important for the health protection of workers who may possibly be exposed to chemicals or agents in the workplace. It is used to help check that health practices are followed and that individuals are kept safe from possible exposures. Biomonitoring is used to assess exposures and to determine the potential health effects or consequent risks. It can also aid in risk management and policy-making as well as in the identification of groups of workers that are at higher risk (Angerer et al, 2007). Another application of biomonitoring involves shedding light on human metabolic response to radiation in vivo without experimental exposure (Angerer et al, 2007).

iThemba LABS, in collaboration with the Radiation Regulatory Authorities in South Africa (the Directorate Radiation Control of the Department of Health and the National Nuclear Regulator) are currently conducting a project to biomonitor radiation workers, which can be done by analysing chromosomal damage e.g. dicentric formation or by counting micronuclei in T-lymphocytes.

Low dose radiation poses a particular problem, as the effects it has on individuals, both in the short term and in the long term, are not fully understood. Moreover, most over-exposure cases involve low doses of ionising radiation (Tucker, 2008). A question that needs to be addressed

regarding low doses is: is there a threshold below which radiation does not induce permanent or harmful aberrations? An adaptive response has been observed at low doses, where exposure at low doses has diminished the effect of exposure to a higher dose. It is important to assess risks at low doses of radiation in relation to occupational exposure (chronic) (Darroudi et al, 2008), because, although chronic exposures result in simpler aberrations, they are more likely to persist as the cells are able to survive with the unrepaired damage. Another difficulty is that biological methods may not be sensitive or accurate enough to detect the damage produced upon exposure to low doses.

1.1.6 Chromosomal radiosensitivity

Radiosensitivity refers to how susceptible an organism or cell is to radiation. Individuals differ in their radiosensitivity, as different cell types may also differ. Lymphocytes are among the most radiosensitive cells in the body, in particular CD8+ cells, which have been shown to be more radiosensitive than other lymphocyte subpopulations (Wilkins et al, 2002). Several factors affect radiosensitivity, some being external, such as the conditions and stresses that a cell is exposed to prior to and/or during radiation exposure. For example, a mixed lymphocyte culture may fare better than separate cultures for different lymphocyte subpopulations because mixed populations may work in conjunction with one another to protect the population; also a mixed culture has probably undergone far less stress than those that were separated (Wilkins et al, 2002). Inherent factors may involve multiple genes, such as those involved in stress response, DNA repair and apoptosis.

Certain population groups have been shown to have an enhanced chromosomal radiosensitivity. Initially, it was shown that chromosomal radiosensitivity existed among patients with syndromes pre-disposed to

cancer, such as Fanconi's anaemia, Ataxia Telangiectasia, Nijmegen breakage syndrome (Sanford et al, 1989; Scott et al, 1999), whereas later it became apparent that chromosomal sensitivity to ionising radiation can be detected not only within these chromosomal fragility syndromes but also in many other cancer prone conditions (Sanford et al., 1989; reviewed in Scott et al., 1999, Baeyens, 2005). Radiosensitivity has been attributed to DNA repair gene defects (Preston, 1980; Parshad et al, 1983), such as mutations in the protein, Artemis, which result in hypersensitivity to agents known to induce DNA DSBs (Ma et al, 2002), defects in cell cycle checkpoint control (Little and Nagasawa, 1985), as well as in chromatin structure differences (Hittelman and Pandita, 1994) and defective apoptosis.

1.2 Cytogenetic tests

Cytogenetic tests can be performed to examine many different types of chromosomal damage. These tests are used in radiation protection (e.g. biological dosimetry) as well as in fundamental radiobiological research (e.g. *in vitro* chromosomal radiosensitivity studies). There are a number of available tests; the most commonly used are the micronucleus assay, the dicentric assay and the Comet assay. The dicentric assay identifies damaged chromosomes in metaphase, where a DSB or a SSB is mis-repaired and rejoined to another chromosome resulting in a chromosome with two centromeres and acentric fragments. The detection of dicentric chromosomes on Giemsa-stained metaphases can be a time-consuming process. Another option is to use chromosomal banding techniques, which make the chromosomes identifiable from one another. However, this test also requires time and skill to ensure accuracy. The comet assay or Single Cell Gel Electrophoresis (SCGE) assay (Singh et al, 1988) involves embedding the cells in agarose, then lysing them and applying an electric current. Undamaged DNA remains tightly organised and associated with proteins making it larger, and unable to move much along the gel. Damaged

DNA is more free to move, and results in a “tail”, which can be visualised using fluorescence. Different damage can be identified from this tail.

1.2.1 The micronucleus assay

Micronuclei appear as smaller versions of the main nucleus in the cytoplasm of interphase cells (Baeyens, 2005), and they are indicators of more persistent cytogenetic damage. They can be formed in two different ways (Figure 3), because of clastogenic events (such as exposure to ionising radiation) or aneugenic events. Clastogenic events pertain to the loss of chromosomal fragments that are a result of unrepaired DNA DSBs; they are, generally, acentric fragments. Regarding aneugenic events, whole chromosomes may lag behind during mitosis and are, consequently, excluded from the main nucleus. In both cases, nuclear membranes form around these chromosomal fragments or whole chromosomes, and they form micronuclei in the cytoplasm. Most spontaneous micronuclei result from aneugenic events and are therefore centromere-positive, whilst clastogenic agents, such as radiation, result in mostly centromere-negative micronuclei.

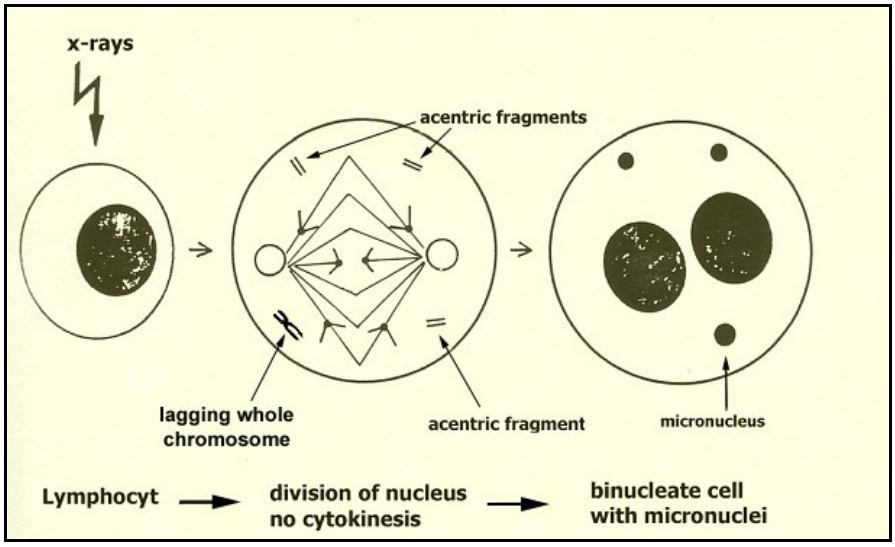

Figure 3: Overview of micronucleus formation (Baeyens, 2005).

The micronucleus assay was developed by Fenech and Morley (1985), and it has since been established and validated as an excellent tool for detecting radiation-induced DNA damage (in the form of micronuclei). The micronucleus assay involves stimulating cell division with the mitogen, phytohaemagglutinin (PHA), but blocks cytokinesis with cytochalasin-B, which prevents the polymerisation of actin filaments. This allows nuclei to divide but prevents completion of cell division. Micronuclei are counted in cells that have undergone a single nuclear division i.e. a binucleated cell.

There are numerous advantages to the micronucleus assay, firstly because it is a simple and easy-to-use technique. It has clearly defined endpoints as shown in Figure 4, which indicates variations on what can be accepted as true micronuclei. It has been adapted to a high-throughput automated process involving the slide scanning system Metafer (Schunck et al, 2004). It is useful in immediate dose assessment. It also fulfils the criteria for a reliable biomonitoring system – 1) blood is an easily collected specimen with little discomfort to the patient, 2) there is a set parameter for detecting the number of micronuclei, and 3) the method is well-established. Reference and limit values may need to be established in many individual and population groups and for different types of ionising radiation.

However, one disadvantage is that the assay cannot distinguish between spontaneous damage and radiation-induced damage in low doses (usually below 0.3 Gy). This is because the number of micronuclei produced is similar to unexposed controls and the micronuclei count is usually quite low. The micronucleus assay can be adapted to be used in conjunction with other techniques, such as Fluorescence *In Situ* Hybridisation (FISH). FISH with a pancentromeric probe coupled with the micronucleus assay is able to distinguish between spontaneous damage and radiation-induced damage in low doses (usually below 0.3 Gy).

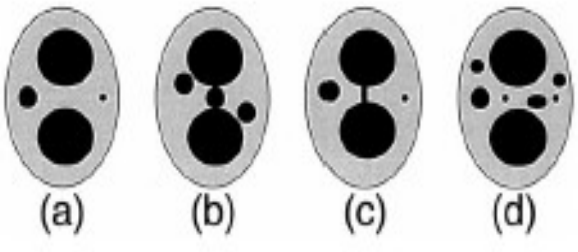

Figure 4: Schematic drawings of binucleated cells with true micronuclei, (a) two micronuclei of different sizes – 1/3 and 1/9 of main nuclei diameter, (b) micronuclei that are touching the main nuclei, but not overlapping it, (c) two micronuclei, and a binucleated cell with a nucleoplasmic bridge, (d) many micronuclei in a binucleated cell (Fenech, 2000).

There is variation among unexposed individuals regarding their micronuclei counts, and various factors can affect them, including age and sex (Fenech et al, 1994; Thierens et al, 1996). Studies have found that micronuclei counts increase with age, and that higher counts are found in females as compared to males (Fenech et al, 1994; Thierens et al, 1996). Pala et al (2008) showed that increasing numbers of centromere-negative micronuclei coincided with increasing doses of ionising radiation, which corroborates the assumption that radiation induces centromere-negative micronuclei.

1.2.2 The micronucleus assay combined with the pan-centromeric probe

The pan-centromeric probe allows clastogenic, centromeric-negative micronuclei, and aneugenic, centromere-positive micronuclei, events to be distinguished. This means that background micronuclei can be distinguished from radiation-induced micronuclei.

As has been stated, micronuclei can form through different mechanisms. The combination of the micronucleus assays with FISH using a pan-

centromeric probe can suggest how the micronuclei form as a result of radiation or not. Figure 5 shows a cell that formed micronuclei either because of genomic instability or a genotoxic agent. It also shows that through the use of the micronucleus assay combined with a pan-centromeric probe, how the micronuclei were formed can be determined. Further analysis of the number of centromeric signals in the CM+MN can possibly offer additional information on the nature of the damage sustained.

A pan-centromeric probe will hybridise to all the centromeres of all the chromosomes, including any in the micronuclei and in the main nuclei. The probe bound in the main nuclei acts as an internal control, and hybridisation is deemed successful if the probe has indeed bound to the centromeres present in the main nuclei. Slides can be visualised by using fluorescence microscopy. Although commercial pan-centromeric probes are available it is more feasible to make an in-house probe. Primarily, it is relatively inexpensive to prepare and makes it more affordable for the laboratory and the patient.

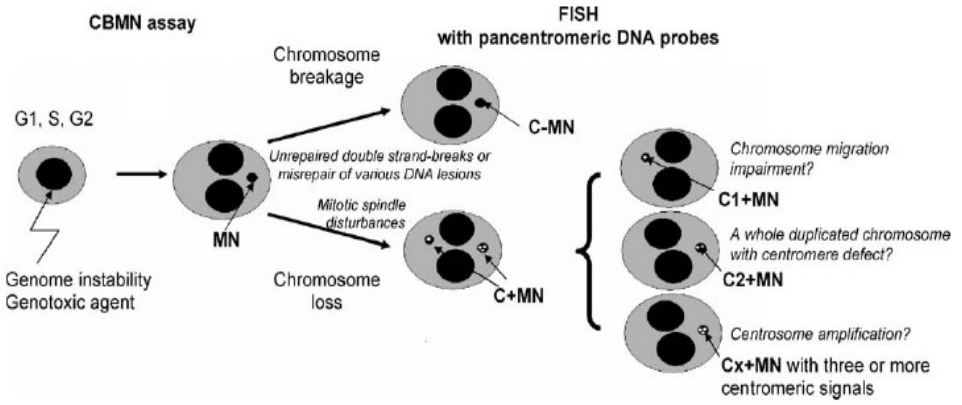

Figure 5: Depiction of the formation of micronuclei through different mechanisms, and the use of the CBMN assay and FISH with pan-centromeric probes to determine how the micronuclei formed (Iarmarcovai *et al*, 2006).

Figure 6 gives an example of a binucleated (BN) cell with a single micronucleus, which has been fluorescently-labelled with a centromeric (red) probe. The nuclei are counterstained with DAPI. The centromeric signals are clear and visible in the main nuclei.

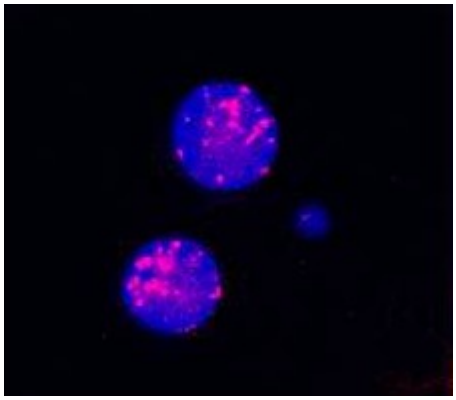

Figure 6: A binucleate cell with a single micronucleus under DAPI (blue nuclei) and fluorescent filters for centromeric probes (red signals).

1.3 Human Immunodeficiency Virus (HIV)

Classification

Group: Group VI (ssRNA-RT)

Family: Retroviridae

Genus: Lentivirus

HIV is a rather large spherical virus with a diameter of about 120 nm. It has two copies of positive single-stranded RNA, which encode the virus's nine genes. The RNA is encapsidated in a conical capsid made from its own viral protein, p24. HIV infects cells involved in the immune system, including CD4+ T-lymphocytes, macrophages and microglial cells. HIV results in immunodeficiency in infected people eventually leading to Acquired ImmunoDeficiency Syndrome (AIDS) when CD4 counts fall below 200 cells/mm^3. HIV infection is treated with Highly Active AntiRetroviral

Treatment (HAART), where the drugs taken target various stages during the HIV life cycle. A number of different drugs with different targets are taken as HIV has a high mutation rate and can develop resistance very quickly. A viral population may have many "quasispecies" with a number of highly heterogeneous sequences (Freed, 2001). HIV also creates and maintains several reservoirs where viruses integrate into cells and remain latent for long periods of time, again allowing the virus to evade the immune system. Cells with latent proviruses may sometimes be infected again. A productive superinfection allows old sequences of the virus to recombine with new ones, leading to one cell producing several strains (Jeeninga et al, 2008).

The life cycle of HIV-1 is depicted in Figure 7, and briefly described here. The virus enters the cell by binding its glycoproteins gp120 to the host cell's CD4 receptor and co-receptor CXCR4 or CCR5. Gp41 catalyses membrane fusion, where the virus and cellular membranes can fuse allowing the viral core to enter into the cytoplasm (Freed, 2001). Fusion requires cholesterol and the receptors to localise at the fusion site for it to occur. Fusion is multistep where firstly the contents of both the membranes are mixed, termed hemifusion, secondly, the fusion pore is formed when gp41 inserts directly into the target membrane and lastly the pore is enlarged (Campbell and Hope, 2008; Freed, 2001). Not all viruses enter the cell through this pathway, many are passively endocytosed by the cell. Upon entry into the cell, the viral genome is uncoated and it is converted into double-stranded DNA via its own pol-encoded enzyme reverse transcriptase (Freed, 2001). The newly transcribed viral DNA is transported actively across the nuclear envelope into the nucleus as part of the PIC (pro-integration complex). The PIC is made up of both viral and cellular proteins that associate with the viral DNA (Freed, 2001). PIC also allows HIV-1 to infect non-dividing cells (Freed, 2004). Another virally encoded protein, integrase, catalyses the integration of the viral DNA into the host cell genome (Freed, 2001). Once

integrated, the provirus can remain latent for several years and acts as a cellular gene. HIV-1 has several novel proteins that are adapted to take advantage of the host cell. Various viral RNAs are transcribed using host machinery. The viral protein TAT acts upon TAR to stimulate transcription and gene expression. Some viral RNAs that are transcribed are not spliced or only partially spliced, and cannot be exported from the nucleus according to host cell mechanisms. One of the first proteins made by the virus is the REV protein, which facilitates the export of these unspliced and/or partially spliced RNAs (Freed, 2001). The viral Gag proteins are responsible for encapsidating the viral RNA genome, the assembly of the virus particle and its release (Freed, 2001). The virus particle buds out of the cell, taking some of the host membrane proteins with it, thereby further evading the host immune response.

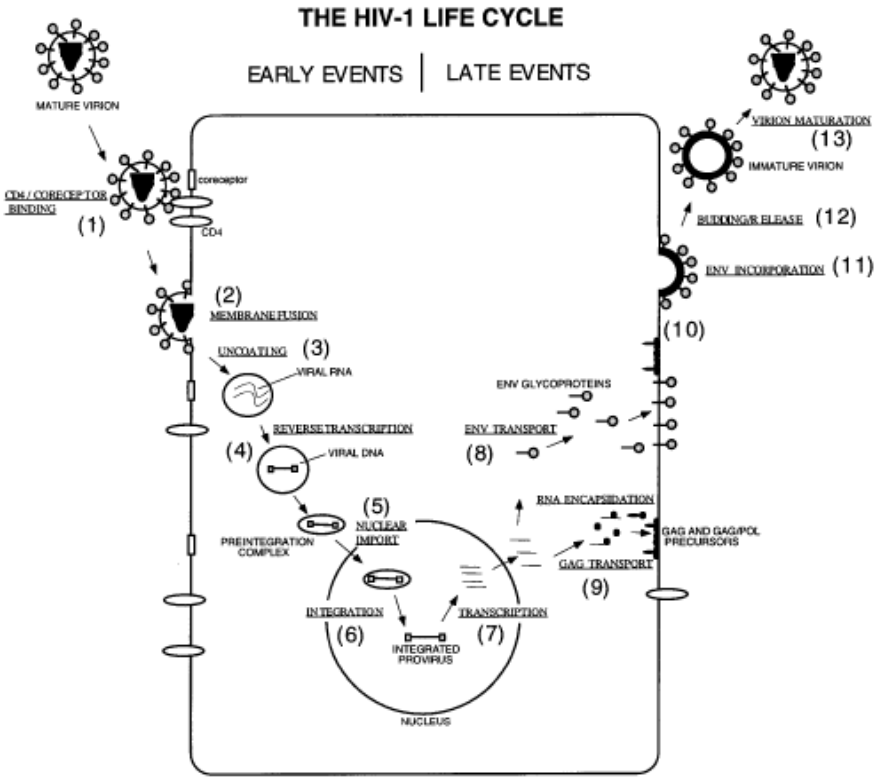

Figure 7: Schematic view of the life-cycle of HIV-1 (Freed, 1998).

HIV infection can result in various processes of the cell being dysregulated. One such example is apoptosis. HIV infection activates the immune system, which remains constantly activated, disrupting the normal expression of proteins involved in the cell cycle. This leads to T-cell dysregulation, and the T-cells become more susceptible to apoptosis (Galati et al, 2002). HIV-1 has also been shown to have enhanced oxidative stress because of reactive oxygen species, which may help explain impairment of T-cell responsiveness and enhanced T-cell apoptosis (Aukrust et al, 2005). Oxidative stress can damage DNA, and one of the lesions formed is 8-oxoG. These lesions are repaired by BER. Disturbed redox balances and increased levels of 8-oxoG lesions are found in HIV+ individuals compared to uninfected controls, with the 8-oxoG levels correlating to the viral RNA copy numbers (Aukrust et al, 2005). It has also been observed that these cells have a reduced capacity to repair this damage because of a downregulation in DNA glycosylase activity for repair (Aukrust et al, 2005). The oxidative stress may be a result of the increased activity of inflammatory cytokines (Aukrust et al, 2005).

There are approximately 33 million people living with HIV worldwide, about 67 % of whom reside in Sub-Saharan Africa. About 90 % of all children with HIV live in Sub-Saharan Africa, and in 2007, 75 % of all AIDS deaths occurred in Sub-Saharan Africa (The AIDS 2008 Impact Report). The five countries with the highest prevalence all lie in southern Africa. South Africa has the most severe epidemic in the world, with approximately 5.7 million of its population infected (about 18 % of its population), and over 350 000 deaths attributed to HIV/AIDS related causes; it is estimated that 1000 AIDS related deaths occur every day in South Africa. South Africa's infection rate is among the worst estimated at 1500 new infections occurring per day (500 000 people newly infected each year). There are a number of contributing factors to the massive epidemic:

poverty, sexual violence, social instability, inequality, low status of women, high levels of sexually transmitted infections, high mobility, limited and uneven access to quality health care and poor leadership in response to the epidemic (The AIDS 2008 Impact Report).

In South Africa, a large proportion of the population is HIV+, and may be in an occupation where exposure to ionising radiation may occur. Also, with HAART and continuing treatment for HIV the epidemic is changing and people are living longer, and they may develop cancer. It is important to ensure that safety criteria are appropriate for all, and that treatment for cancer can be catered for a more representative population.

Biomonitoring can identify individuals that are at higher risk with regards to radiation exposure(Angerer et al, 2007), such as in the unique setting of South Africa where a significant proportion of the population is HIV positive and in a situation where occupational exposure to ionising radiation may occur. Recently published data (Baeyens et al, 2010) has indicated that HIV positive individuals may be more radiosensitive than HIV negative individuals, and would therefore be more at risk to radiation exposure in the workplace. Within South Africa's unique population, the relationship between HIV and radiosensitivity needs to be further explored, in order to better assess the risks involved with regards to the use of ionising radiation both in the workplace and in radiation therapy.

Aim

The general aim of this study was to develop a human DNA pan-centromeric marker in order to differentiate between spontaneous micronuclei and radiation-induced micronuclei. It is especially important to understand what occurs in response to exposure to low doses of ionising radiation. The majority of accidental exposures in the workplace occur in the low dose range, and the sensitivity of the tests currently used is restricted to 0.2 Gy – 0.3 Gy. The combination of a pan-centromeric marker with the micronucleus assay would further refine the low dose radiation-induced damage detection. The use of a combined automatic micronucleus pan-centromeric probe scoring system would facilitate the development of biomonitoring radiation workers. In cases of massive radiation accidents, this technique will allow an accurate assessment of exposure. A financially viable and time efficient method for developing and using a pan-centromeric probe needs to be explored.

Objectives

- Evaluate and optimise two methods used to create the pan-centromeric probe, and compare the two probes with one another and with a commercial probe after hybridisation to metaphase slides. Based on these results one method was selected.
- Apply the selected probe in a biological dose-dependent assay, where lymphocytes from healthy donors are irradiated with different doses of gamma radiation, and the total number of micronuclei, the number of micronuclei with or without a signal are scored.
- Compare automated and semi-automated scoring of micronuclei on the MetaFer system.
- Apply the probe to evaluate the base line number of micronuclei in HIV-positive and HIV-negative donors.
- Establish a biological dose-dependent assay in HIV-positive and HIV-negative lymphocytes irradiated at different doses.

CHAPTER TWO – MATERIALS

2.1 Sample collection

Fresh blood samples were collected by means of venepuncture in lithium-heparin or EDTA tubes. Signed informed consent was received from all volunteers. Data regarding age, smoking habits and gender were also collected, as age, smoking and gender can influence the micronucleus values. Samples were all coded. This study was approved by the Human Research Ethics Committee, University of the Witwatersrand, Johannesburg, South Africa (M090475).

2.1.1 Control samples

Twenty blood samples were collected from healthy donors. Donors were from the Somatic Cell Genetics Unit, Department of Molecular Medicine and Haematology, University of the Witwatersrand, South Africa and at the Department of Basic Medical Science, University of Ghent, Belgium. Blood samples for culturing micronucleus assays and metaphase cultures were collected in Li-heparin tubes. Blood was also collected for DNA extractions from healthy male donors in EDTA tubes. Male donors were used so that the centromeres of all autosomal chromosomes as well as the X and Y chromosomes, were acquired. Ten samples were used from healthy donors for culturing purposes, and all cultures were performed in duplicate, and the rest were used as controls in the HIV study.

2.1.2 HIV samples

Thirty-five blood samples were collected in Li-heparin tubes from patients at the HIV centre, Helen Joseph Hospital, Johannesburg, South Africa. Data regarding CD4 counts was collected from the patients and samples were excluded if their CD4 counts fell below 200 cells/mm^3 . Previous data

(Baeyens et al, 2010) has shown that cultures from HIV positive samples with a CD4 count below 200 cells/mm^3 produce too few cells to adequately perform a MN assay. Samples were also excluded if the patients were on ARV treatment, as the treatment could interfere with the micronucleus assay. Nineteen HIV+ samples and thirteen HIV- samples were used for the first part of the HIV study, and eight HIV+ samples and four HIV- samples were used for the second part of the study.

2.2 Product list (see Appendix A)

CHAPTER THREE – METHODS

3.1 Micronucleus assay

Two methods were used for the micronucleus tests. Method 1 was used in South Africa (Somatic Cell Genetics Unit, Department of Molecular Medicine and Haematology, University of the Witwatersrand) and Method 2 was used in Belgium (Department of Basic Medical Science, University of Ghent). The differences in the methods were dependent on what was available in the different laboratories, and how the irradiations were performed, and did not affect the validity of the results.

3.1.1 Method 1

4.5 ml of pre-warmed complete medium (Appendix A) was added to a culture flask (25 cm^3). 500 µl of whole blood was added to this. The cultures were irradiated or mock-irradiated. 100 µl of phytohaemagglutinin (PHA) was added to the cultures. The cultures were incubated at 37 °C, upright, 5 % CO_2. Twenty-three hours later, 20 µl of cytochalasin B (Appendix A) was added to the culture. Seventy hours after adding PHA, the cultures were harvested. The blood mixture was transferred to a 15 ml tube and centrifuged at 1000 rpm for 8 minutes. The supernatant was removed. 7 ml of cold KCl (Appendix A) was added dropwise while vortexing. The tubes were centrifuged at 1000 rpm for 8 minutes. The supernatant was removed and 7 ml of cold 4:1:5♦ methanol:acetic acid:Ringer (Appendix A) fixative was added dropwise while vortexing. Ringer acts as a buffer preventing the lymphocytes from bursting. The tubes were stored at 4 °C overnight. The following day, the cultures were further fixed. The tubes were centrifuged at 1000 rpm for 8 minutes. The supernatant was removed. 5 ml of 4:1 methanol:acetic acid was added while vortexing. This was repeated until the solution was clear. The samples were centrifuged at 1000 rpm for 8 minutes. The supernatant was removed, leaving enough fixative (usually about

500µl♣) to resuspend the pellet. The tube was vortexed to resuspend the pellet, and 40 µl of the suspension was dropped onto a clean glass slide (cleaned in methanol) and spread as much as possible by tilting the slide back and forth. The slides were air-dried and kept at room temperature.

♦ 10:1:11 methanol:acetic acid:ringer fixative was used when slides were prepared for manual scoring. Subsequently, 4:1 methanol:acetic acid fixative was replaced with 10:1.

♣ samples that were manually scored were concentrated more and spread out less

3.1.2 Method 2

3 ml of pre-warmed complete medium (Appendix A) with 10 % FCS was added to a culture flask, and 1.5 ml was added to a round-bottomed tube. 500 µl of whole blood was added to this. The cultures were irradiated or mock-irradiated. The contents of the tube were transferred to the culture flask containing the 3 ml of medium. 100 µl of PHA was added to the cultures. The cultures were incubated at 37 °C, upright, 5 % CO_2. Twenty-three hours later, 20 µl of cytochalasin B was added to the culture. Seventy hours after adding PHA, the cultures were harvested. The blood mixture was transferred to a 15 ml tube and centrifuged at 1000 rpm for 8 minutes. The supernatant was removed. 7 ml of cold KCl was added dropwise while vortexing. The tubes were centrifuged at 1000 rpm for 8 minutes. The supernatant was removed and 7 ml of cold 4:1:5 methanol:acetic acid:ringer fixative was added dropwise while vortexing. The tubes were stored at 4 °C overnight. The following day, the cultures were fixed. The tubes were centrifuged at 1000 rpm for 8 minutes. The supernatant was removed. 5 ml of 4:1 methanol:acetic acid was added while vortexing. This was repeated until the solution was clear. The samples were centrifuged at 1000 rpm for 8 minutes. The supernatant was removed, leaving enough fixative (usually about 500 µl) to resuspend the pellet. The tube was vortexed to resuspend the pellet, and 40 µl of the suspension was dropped onto a clean glass slide

(cleaned in methanol) and spread as much as possible by tilting the slide back and forth. The slides were air-dried and were kept at room temperature.

3.2 Classic cytogenetic test for chromosomal aberrations

Metaphase preparations were done to test whether the pan-centromeric probes were hybridising to all centromeres of all chromosomes.

4.5 ml of complete medium (Appendix A, complete medium for method 1) was added to a culture flask. 500 µl of whole blood was added to this, and 100 µl of PHA was also added. The culture was incubated at 37 °C, 5 % CO_2, horizontally with the caps slightly open. Forty-three hours later, 100 µl of colcemid (Gibco) was added to the cultures to stall the cell division at metaphase. Forty-seven hours after start-up the cultures were harvested. The blood mixture was transferred to a 15 ml tube and centrifuged at 1000 rpm for 8 minutes. The supernatant was removed. 5 ml of KCl, prewarmed to 37 °C, was added dropwise while vortexing. The tubes were incubated at 37 °C for 15 minutes. They were centrifuged at 1000 rpm for 8 minutes. The supernatant was removed and 5 ml of cold 3:1 methanol:acetic acid fixative was added while vortexing. This was repeated until the solution was clear, then stored at 4 °C. The samples were centrifuged at 1000 rpm for 8 minutes. The supernatant was removed, leaving enough fixative to resuspend the pellet. The tube was vortexed to resuspend the pellet, and 50 µl of the suspension was dropped onto a clean glass slide (cleaned in methanol) from 30 cm. The slides were air-dried and were kept at room temperature.

3.3 Irradiation procedures

Irradiations were performed at Medical Physics, Charlotte Maxeke Hospital, South Africa and at the Institute for Nuclear Sciences (INW), Belgium. Safety procedures were followed for all irradiations, including the wearing of personal radiation dosimeters. Irradiations were performed by a competent technician.

3.3.1 Dose Response study

Doses in the dose response study were 0.05 Gy, 0.1 Gy, 0.2 Gy, 0.3 Gy, 0.5 Gy, 0.75 Gy, 1 Gy, 2 Gy. Samples were also mock-irradiated as controls. Gamma radiation from a cobalt-60 (Co-60) source was used. Ten samples were collected in total, and perfomed in duplicate.

At the INW, the irradiations for the doses 0.05 Gy – 0.2 Gy were performed in a heated water bath (37 °C) 30 cm from the source at a dose rate of 0.01 Gy/min; the irradiations for the doses 0.3 Gy – 2 Gy were performed in a heated water bath (37 °C) at a dose rate of 0.32 Gy/min. The irradiations carried out at Medical Physics, Charlotte Maxeke Hospital, Johannesburg, South Africa were performed in a water bath at ambient temperature at a dose rate of 1.52 Gy/min.

3.3.2 HIV study

HIV samples were irradiated at Medical Physics, Charlotte Maxeke Hospital, South Africa with a 6 MV photon beam from a medical linear accelerator (Siemens Healthcare, Erlangen, Germany). The HIV study comprised two parts. HIV samples collected for the first part of the study were irradiated at doses of 2 Gy and 4 Gy, and mock-irradiated. The culture flasks were fixed at a depth of 11.5 cm in a water bath (30 cm × 30 cm × 30

cm) and placed at the isocentre of the beam, where the field size was 10 cm × 10 cm. The doses were delivered at a dose rate of 1.33 Gy/min. These irradiated samples were manually scored. The samples collected during the second part of the study were not irradiated and were scored semi-automatically.

3.4 Slide Staining

Slides were stained depending on what they were to be used for. Slides stained with acridine orange were scored manually for micronuclei, and slides stained with DAPI alone were scored automatically on the MetaFer for micronuclei.

3.4.1 Acridine Orange Staining

Slides were immersed in acridine orange working solution (Appendix A) for one minute, rinsed in distilled water, and immersed in acridine orange buffer for one minute. The slides were removed from the buffer, and 20 µl of buffer was dropped onto the slides to avoid drying out. A glass coverslip was carefully placed over the slide avoiding air bubbles, and sealed with rubber cement. The slides were manually scored for micronuclei within three days (see section 3.6). Acridine orange stains the cytoplasm orange and the nuclei green.

3.4.2 DAPI Staining

Slides were stained with a drop of Vectashield with DAPI (Vector Labs). The nuclei were stained blue, as DAPI intercalates the DNA. These slides were scored automatically on the Metafer 10 × objective (see section 3.6).

3.5 *F*luorescent I*n* S*itu H*ybridisation (FISH)

The pan-centromeric probe was applied to micronucleus and metaphase slides by means of FISH methodologies. Slides were dehydrated prior to hybridisation in order to maintain chromosome morphology and wash away any fixative still present on the slide. Some pretreatments were tried in order to obtain optimal FISH results, and are described below. The methods used to create the pan-centromeric probes are described. Hybridisation and washing, methods are described below, were performed on these slides, and where indicated the protocols for the commercial STARFISH© denaturing solution pan-centromeric probe are also described.

3.5.1 Slide preparation

Slides were dehydrated in an ethanol (Merck) series (70 %, 90 %,100 %) for 5 minutes each and aged overnight at room temperature.

Pretreatments

Various pretreatments were tried in order to improve hybridisation and lower background. The desired result was to have no cytoplasm, which may restrict the pan-centromeric probe from entering the nucleus and hybridising to the chromosomes. The following pretreatments were tried:

3.5.1a) RNase only pretreatment

The slides were incubated with 100 µg/ml RNase (Roche) for one hour at 37 °C, then washed in 2 × SSC for 5 minutes followed by another 5-minute wash in PBS. The slides were dehydrated in a room temperature ethanol series. Controls received no treatment. FISH was performed on these slides.

3.5.1b) RNase and pepsin pretreatment I

The slides were incubated with 100 µg/ml RNase (Roche) for one hour at 37 °C, then washed in 2 × SSC for 5 minutes followed by another 5-minute wash in PBS. The slides were treated with pepsin for 2 minutes in a moist chamber at room temperature. The slides were washed in PBS for 5 minutes, then dehydrated in a room temperature ethanol series. Controls received no treatment. FISH was performed on these slides.

3.5.1c) RNase and pepsin pretreatment II

Slides were treated with 100 µg/ml RNase / 2 × SSC for thirty minutes at 37 °C in a moist chamber, then washed three times in 2 × SSC at room temperature for five minutes each. The slides were dehydrated in a room temperature ethanol series and air-dried. The slides were incubated with 0.001 % pepsin / 0.01 M HCl at 37 °C for 5 minutes. The slides were washed in PBS for 5 minutes, and dehydrated in a room temperature ethanol series. The slides were post-fixed in postfixation buffer (Appendix A), followed by a 5-minute wash in 4 % paraformaldehyde (Appendix A), and a 5-minute wash in PBS. The slides were dehydrated in room temperature ethanol series. FISH was carried out on these slides.

3.5.1d) Pepsin only pretreatment

The slides were washed for two minutes in a pepsin solution at 37 °C. They were then fixed in 1 % formaldehyde followed by two washes in 2 × SSC for 5 minutes each. They were dried and dehydrated in a room temperature ethanol series. FISH was performed on the slides.

3.5.2 Probe preparation

Two different methods are used to make a pan-centromeric probe; the first utilises a human DNA sequence clone called p82H, and the second involves making a synthetic probe from human DNA with primers designed to target the centromeres. Both products are labelled by means of nick translation with fluorescent SpectrumOrange dUTPs to be used as a probe in FISH. A commercial probe, STARFISH© pan-centromeric probe, was compared with the made probes according to their hybridisation to metaphase slides.

3.5.2.1 p82H probe

p82H is a 2.4 kb human DNA sequence. It is a member of the alphoid repeated sequence family. The p82H clone hybridises to the centromeres of all chromosomes (Mitchell et al, 1985; Aleixandre et al, 1987). The p82H plasmid is grown in *Escherichia coli* and extracted using a plasmid extraction kit (Qiagen).

Bacterial culture

A single bacterial colony from an agar plate was planted in 5 ml of Luria Broth (LB) medium (Appendix A) containing 1 mg/ml ampicillin using sterile techniques. This starter culture was incubated for 6-8 hours at 37 °C on a shaking incubator. The turbidity, indicating bacterial growth, of the medium was observed after the incubation period. Once the turbidity was sufficient, the starter culture was diluted in 200 ml of fresh LB medium in an Erlenmeyer flask stoppered with cotton wool and tinfoil, and incubated for approximately 16 hours at 37 °C on the shaking incubator under sterile conditions. After 16 hours, the cultures were transferred to 50 ml NUNC tubes and centrifuged at 6000 × g for 15 minutes. The supernatants were discarded, and the pellets could be used immediately for plasmid extraction described below. Glycerol stocks were made from the starter culture by adding 800 µl of the starter culture to 200 µl of glycerol, mixing and storing

at −70 °C. These could be used to start up new cultures for plating.

Plasmid extraction

Plasmids were extracted using Qiagen's Plasmid Midi Kit as per protocol (see Appendix A). Briefly, the pellet was resuspended in 4 ml Buffer P1. 4 ml of Buffer P2 was added, and mixed by inverting six times. The solution turned a bright blue colour, and was homogeneous when completely mixed. The solution was incubated at room temperature for five minutes. 4 ml of Buffer P3 was added, and mixed by inversion. A white precipitate formed and the solution became less viscous; the solution also lost its blue colour. This was incubated on ice for fifteen minutes. The solution was centrifuged at 20000 × g for thirty minutes at 4 °C, and the supernatant, containing the DNA, was transferred to a new 50 ml NUNC tube, which was centrifuged again at 20000 × g for fifteen minutes at 4 °C to remove excess precipitate. The supernatant was transferred to the QIAGEN-tip 100, which had been equilibrated by allowing 4 ml of Buffer QBT to flow through it, and allowed to flow through the tip. The QIAGEN-tip 100 was then washed twice with 10 ml of Buffer QC. The DNA was eluted with 5 ml Buffer QF preheated at 65 °C. The DNA was precipitated as follows. 3.5 ml of isopropanol (room temperature) was added to the eluted DNA, and centrifuged at 15000 × g for 30 minutes at 4 °C. The supernatant was discarded. 2 ml of 70 % ethanol (room temperature) was added to wash the pellet. The tube was centrifuged at 15000 × g for 10 minutes. The supernatant was carefully decanted. The pellet was air-dried for 5-10 minutes before adding 100 µl of TE Buffer (Promega) to redissolve the pellet. This was left at room temperature to dissolve, then stored at −20 °C. 2 µl of the extracted DNA was electrophoresed on a 2 % agarose gel against lambda DNA to determine if the extraction was successful, and evaluate the quantity of plasmid DNA (Figure 16, Appendix B).

3.5.2.2 Synthetic probe

Specific primers used can isolate and amplify the centromeric DNA (Weier et al, 1991). For this method, male DNA has to be used to obtain X, Y and autosomal centromeres. The PCR product can then be purified.

DNA extraction: In-house phenol-chloroform method

Blood collected in EDTA tubes was centrifuged at 1500 rpm for 10 minutes at room temperature. The serum was removed with Pasteur pipettes. 1 ml of the buffy coat was aspirated up and added to 5 ml (1:5 ratio) of ice-cold red blood cell lysis buffer (Roche) in a 15 ml tube. This was incubated on ice for 15 minutes, vortexing every 5 minutes to lyse the red blood cells, indicated by the solution becoming less opaque. It was then centrifuged at 1500 rpm for 10 minutes at 4 °C. The supernatant was removed from the small white pellet at the bottom of the tube. 2 ml of red blood cell lysis buffer (at room temperature) was added to the pellet and vortexed. The tube was centrifuged at 1500 rpm for 10 minutes at 4 °C. The supernatant was removed as much as possible. 4 ml of proteinase-K lysis buffer (Appendix A) was added to the pellet and aspirated to resuspend. 320 µl of 10 mg/ml proteinase-K (Roche) was added and mixed well with the solution ensuring that it was homogeneous. The solution was incubated at 56 °C for one hour, mixing every fifteen minutes to digest proteins. 4 ml of phenol (Sigma-aldrich) and 4 ml of chloroform were added to the solution and vortexed vigorously for one minute. The solution was centrifuged at 6000 rpm for 10 minutes at 4 °C. It separated into three layers, and the top layer, containing the DNA, was transferred to a new tube. 2 ml of phenol and 2 ml of chloroform were added to this, vortexed and centrifuged at 6000 rpm for 10 minutes at 4 °C. The top layer was transferred to a new tube, and 4 ml of chloroform was added to it, vortexed and centrifuged at 6000 rpm for 10 minutes at 4 °C. This was repeated until the solution was clear and no more white precipitate was present. The top layer was transferred to a new tube,

and 2.5 × the volume of ice-cold 100 % ethanol was added to the solution in order to precipitate the DNA. It was centrifuged at 6000 rpm for 10 minutes at 4 °C, and the supernatant was discarded. 2.5 ml of ice-cold 70 % ethanol was added to the pellet and centrifuged at 6000 × g for 10 minutes at 4 °C. The supernatant was discarded and the pellet air-dried for about 30 minutes upside down. The pellet was resuspended in 50 µl 1 × TE buffer, and left at room temperature to dissolve overnight. The concentration was determined on a NanoDrop spectrophotometer.

***P*olymerase *C*hain *R*eaction (PCR)**

PCR was set up on ice and performed on thermocycler, Eppendorf, with the primers:

Forward primer: 5'-GAA GCT TAA CTC ACA GAG TTG AA-3' (Weier et al, 1991);

Reverse primer: 5'-GCT GCA GAT CAC AAA GAA GTT TC-3' (Weier et al, 1991).

Table 1: Reagent concentrations and volumes for PCR

REAGENT	STOCK CONCENTRATION	FINAL CONCENTRATION	VOLUME (µl) × 1
DNA		250 ng	
Forward primer (Operon biotechnologies)	100 µM	1.2 µM	1.2
Reverse primer (Operon biotechnologies)	100 µM	1.2 µM	1.2
10 × NH_4 reaction buffer (Bioline)	10 ×	1 ×	10
$MgCl_2$ (Bioline)	10 mM	1.6 mM	16
dNTP mix (Promega)	10 mM	100 µM	1
BIOTAQ DNA polymerase (Bioline)	5 U/l	5 U	1
dH_2O	-	-	Up to 100
TOTAL			**100**

The PCR reaction was performed on the following programme (Weier et al, 1991):

95 °C	10 minutes	
96 °C	1 minute	30 cycles
45 °C	1 minute	
72 °C	1 minute	
72 °C	5 minutes	
4 °C	∞	

5 µl of the PCR product was electrophoresed on a 2 % agarose gel against a 100 bp DNA ladder (Fermentas). The reaction was deemed successful when two bands were visible at the sizes of 175 bp and 345 bp (Figure 18, Appendix B). The remainder of the reaction was stored at 4 °C.

PCR purification

PCR purification was performed by means of PCR purification kits following their protocols.

1) BioSpin PCR amplicon purification kit (South Africa)

Two volumes of Binding Buffer were added to one volume of PCR product, and mixed by vortexing. The solution was added to the column, inserted into a collection tube, and centrifuged for one minute at 6000 × g binding the sample to the column. The flowthrough was discarded, and the column reinserted into the same collection tube. 650 µl of Wash Buffer was added to the column, and centrifuged at 12000 × g for one minute. The flowthrough was discarded and 650 µl of Wash Buffer was added again, and centrifuged at 12000 × g for one minute. The flowthrough was discarded and the column dried by centrifuging it at 12000 × g for one minute. The column was transferred to a 1.5 ml microcentrifuge tube. 30 µl of purified molecular grade water was added to the column and incubated for one minute at room temperature. It was then centrifuged at 12000 × g for one minute to elute the

DNA. The column was discarded and the eluted DNA stored at −20 ºC. The concentration of the DNA was determined using a spectrophotometer.

2) High Pure PCR Product Purification Kit (Roche) (Belgium)

The PCR product (approximately 100 µl) was transferred to a 1.5 ml microcentrifuge tube. 500 µl of Binding Buffer was added to the product and mixed well by means of aspirating up and down. This solution was transferred to a High Pure Filter Tube (polypropylene tubes with two layers of glass fibre fleece) inserted into a Collection Tube (polypropylene tubes), and centrifuged for sixty seconds at maximum speed on a microcentrifuge at room temperature. The flowthrough was discarded from the Collection Tube, and the Filter Tube reinserted into the same Collection Tube. 500 µl of Wash Buffer was added to the Filter Tube, and centrifuged for sixty seconds at maximum speed. The flowthrough was discarded, and the Filter Tube reinserted into the same Collection Tube. 200 µl of Wash Buffer was added to the Filter Tube, and centrifuged for sixty minutes at maximum speed. The flowthrough and Collection Tube were discarded. The Filter Tube was inserted into a new 1.5 ml microcentrifuge tube. 50 µl of Elution Buffer was added to the Filter Tube, and centrifuged for sixty seconds at maximum speed. The Filter Tube was discarded and the eluted DNA was stored at −20 ºC. The concentration of the eluted DNA was determined on a spectrophotometer.

3.5.2.3 Direct labelling

Labelling by nick translation

The labelling reaction was set up as follows:

Table 2: Reagent volumes for the labelling reaction.

REAGENT	VOLUME (µl) ×1
Nick translation buffer (Appendix A)	10
0.1 M β-mercaptoethanol (Sigma-aldrich)	10
dNTP mix (Appendix A)	8
DNA	1-2 µg
DNA polymerase I (Promega)	3
DNase I (Roche) dilution[1] [2]	1
dH_2O	Up to 100
TOTAL	**100**

[1]The DNase I dilution used for the p82H probe was 5.5 µl stock in 1ml distilled water

[2]The DNase I dilution used for the synthetic probe was 0.5 µl stock in 1ml distilled water.

The reaction took place at 15 °C for 30 minutes with regards to the synthetic probe, or for two hours for the p82H probe.

8 µl of the reaction was denatured at 96 °C for three minutes in a thermocycler and electrophoresed against a 100 bp DNA ladder (Fermentas). The reaction was successful when the DNA smear was between 200 bp – 500 bp (Figures 17 and 19, Appendix B). If the reaction was unsuccessful, one microlitre of the DNase I dilution was added to the remainder of the reaction and the reaction was executed at 15 °C for 45 minutes, in the case of the p82H probe. Rarely did the synthetic probe require to be redigested, but when it was necessary the reaction was redigested for 10 – 15 minutes.

Enzymatic Inactivation

The reaction was stopped by inactivating the enzyme. This was accomplished by adding 3 µl of 0.5 M EDTA and 1 µl 10 % Sodium Dodecyl Sulphate (SDS). The tubes were placed at 65 °C for fifteen minutes in a thermocycler.

Probe precipitation

2 µl of 10 mg/ml herring sperm DNA (Promega), which binds repetitive DNA, was added to the reaction. 3 M NaAc3 was added to the reaction in the volume of 10 % of the total volume, and ice-cold 100 % ethanol was added at 2.5 × the total volume. The probe was placed at −70 °C overnight. The following day the probe was centrifuged at 13000 rpm for 30 minutes at 4 °C. The supernatant was discarded and 200 µl of ice-cold 70 % ethanol was added. It was centrifuged at 13000 rpm for 10 minutes at 4 °C. The supernatant was discarded and the pellet was briefly air-dried. Sixty microlitres of hybridisation buffer were added to the pellet, which was left to dissolve overnight at room temperature.

3.5.3 Hybridisation

Slides were denatured in denaturing solution (Appendix A) heated to 76 °C for five minutes, then dehydrated in an ice-cold ethanol series (70 %, 90 % and 100 %) for five minutes each. The probe was denatured at 76 °C for five minutes, and put on ice. 7.5 µl of the probe was applied to a coverslip, cleaned in 100 % ethanol and with a soft tissue. Each slide was placed on the coverslip, and sealed with rubber cement (Fixogum, Marabu). The slides were then incubated at 37 °C in a moist chamber overnight.

STARFISH© commercial pan-centromeric probe hybridisation (as per protocol)

Slides were denatured in 70 % formamide / 2 × SSC at 70 °C for two minutes, then placed in ice-cold 70 % ethanol for five minutes followed by ice-cold 90 % and ice-cold 100 % ethanol for five minutes each. The probe was denatured at 85 °C for ten minutes, and then placed on ice. Ten microlitres of the commercial probe was added to each slide, sealed with a coverslip and rubber cement. The slides were then incubated at 37 °C for

about 16 hours in a moist chamber.

3.5.4 Washing

The rubber cement was carefully removed from the slides, which were then rinsed in 50 % formamide allowing the coverslip to slip off (or the coverslip was gently tapped off) each slide. The slides were washed three times in 50 % formamide heated to 46 °C for ten minutes each, followed by a 10-minute wash in 2 × SSC heated to 46 °C and a five minute wash in 2 × SSC with 0.1 % Tween heated to 46 °C. The slides were removed from the solutions, and mounted with Vectashield containing DAPI, which would counterstain the nuclei (blue) by intercalating with the DNA.

When Vectashield with DAPI was not available, the slides were counterstained in a 2 × SSC solution containing 0.2 µg/ml DAPI (Merck) for fifteen minutes at room temperature, followed by a two minute wash in 2 × SSC with 0.1 % Tween. The slides were then mounted with Vectashield.

STARFISH© commercial pan-centromeric probe washing (as per protocol)

The rubber cement was removed, and the slides rinsed for 5 minutes at 37 °C in 2 × SSC. The coverslips were then removed. The slides were washed twice in 50 % formamide / 2 × SSC for 5 minutes each at 37 °C, then washed twice in 2 × SSC for 5 minutes each, and then counterstained and mounted with Vectashield with DAPI.

3.6 Scoring

Slides were scored microscopically, based on distinct criteria described below. Slides could be scored manually or automatically on the MetaFer system.

3.6.1 Manual scoring

Scoring criteria

Distinct criteria were laid down for scoring the micronuclei (Fenech, 2000). Nuclei were scored if they had undergone a single nuclear division i.e. a binucleated cell. Nuclei were approximately of the same size, and were distinct from one another. Micronuclei were similar in shape to the main nuclei with similar staining. The micronuclei ranged in size from 1/16 to 1/3 of the size of the main nuclei.

a) Acridine Orange stained slides

Nuclei were stained green/yellow with a clear orange cytoplasm with acridine orange. Slides were scored under the DAPI filter on 100 × objective (oil immersion) on an Olympus BX41 microscope. At least 500 binucleated cells were scored per slide (Fenech, 2000).

b) FISH stained slides

Metaphase and micronucleus slides were observed under 100 × objective (oil immersion) on an Olympus BX61 microscope. A triple filter was used to observe if the pan-centromeric probe had bound. In the case of the metaphase slides, metaphases were observed for the pan-centromeric probe binding onto all chromosomes. Images were taken and processed using CytoVision. With regards to the micronucleus slides, cells were scored if signals were clearly present in the main nuclei.

3.6.2 Automated and Semi-automated scoring

Micronuclei were automatically scored with the automated slide scanning system, Metafer. The system is comprised of a computer containing the appropriate software, a motorised microscope (Axioplan 2 Imaging E MOT (Carl Zeiss)) with motorised scanning stage (Marzhauser) and a camera attached for image acquisition. The slide is scanned by moving it in a pattern in reference to a fixed objective lens of a microscope. The field is scanned for any objects of interest (in this case, binucleated cells). If any objects are found, they are analysed and images are taken and stored in a gallery. The image gallery can be viewed later to review and correct if necessary (Schunck et al, 2004).

a) Automated scoring

Metafer MicroNuclei is the system for detecting micronuclei. The system finds binucleated cells stained with a single nuclear stain (e.g. DAPI) under fluorescence (it can also be performed with other nuclear or cytoplasmic stains and with transmitted light). Images are taken of binucleated cells fulfilling the criteria and scored for the presence or absence of micronuclei (Schunck et al, 2004). The micronucleus slides were scored automatically under a 10 × objective using the DAPI filter based on the following MSearch classifier settings (Willems et al, 2010):

Table 3: Classifier setting for the MetaFer, MSearch program.

	Classifier for the binucleated cells	Classifier for the micronuclei
Object threshold (%)	15	7
Minimum area (μm^2)	80	1.00
Maximum area (μm^2)	1000.00	40.00
Maximum relative concavity depth	0.160	0.700
Maximum aspect ratio	1.370	1.700
Maximum distance (μm)	25	25
Maximum area asymmetry (%)	80	
Region of Interest radius (μm)	30	
Maximum object area in region of interest (μm^2)	35	

The *object threshold* separates objects from the background. If the object is accepted as such it is analysed for various features as follows. The *minimum* and *maximum area* defines how small or large an object can be for it to be accepted as a nucleus or micronucleus. The *maximum relative concavity depth* defines how concave a nucleus or micronucleus can be. Both are convex having only small concave areas. The specified limit is relative to the nucleus or micronucleus diameter respectively. The *maximum aspect ratio* discriminates round objects from elongated ones by comparing the axes with one another. The *maximum distance* limits how far two nuclei can be from one another to be accepted as being part of the same cell (distances from the respective centres); it also limits how far a micronucleus can be from the centre of the region of interest (R.o.I.) to be included in the cell. The *maximum area asymmetry* regulates how different in size two nuclei can be from one another, thereby rejecting nuclei of neighbouring cells that lie close together. The *region of interest (R.o.I.) radius* defines the area around the two nuclei that is scanned for other objects. Its centre lies in the middle of a connecting line between the centres of the nuclei. The *maximum object area in R.o.I.* defines how large an object in the R.o.I. can be before the cell is rejected. Therefore cells with more than two nuclei within the R.o.I. can be rejected (Schunck et al, 2004; MetaFer manual, 2005).

Images were taken of the binucleated cells. MSearch was executed with a sensitivity of 90 % (9 out of 10), over a search window of 90 % of the slide (from the centre of the slide) and scored 1000 to 2000 binucleated cells.

b) Semi-automated scoring

The binucleated cells were reviewed in the image gallery. Only binucleated cells having micronuclei were selected from those found in MSearch. These cells were scanned again under the AutoCapt programme, with a DAPI filter and Spectrum Orange filter and using the 40 × objective. Images were taken

of these cells. The images were scored for centromere positive and negative micronuclei. Centromere positive micronuclei were scored as such when the signal was clear and comparable to those in the nuclei.

3.7 Statistical analysis

GraphPad Prism 4 was used for the analysis of the data, using the Wilcoxon signed rank test and the Mann-Whitney test. Confidence intervals were set at 95 % for both tests.

CHAPTER FOUR – RESULTS

4.1 Probe optimisation

The preparation of the pan-centromeric probes needed to be optimised. The methods were adjusted in several ways, which are described below for both the p82H probe and the synthetic probe.

4.1.1 p82H probe

Bacterial culture

Different amounts of starter cultures were used, including 2 ml, 5 ml and 10 ml, and a 5 ml starter culture was found to provide optimal growth. The starter cultures were diluted in larger amounts, and it was found that 200 ml gave sufficient growth for greatest extraction and yield.

Plasmid extraction

Throughout the plasmid extraction, samples were taken at different stages i.e. from the filtrate of the Buffers P1, P2 and P3, from the flow-through of Buffer QBT, from the filtrate after the washes with Buffer QC, and from the eluate (after Buffer QF). The different steps of the extraction were checked to ensure no DNA was being lost during the extraction by means of electrophoresis on a 2 % agarose gel, and no DNA was lost during the extraction. In order to see if increasing the amounts of Buffers P1, P2 and P3 enhanced the amount of DNA yield, 8 ml and 10 ml of the Buffers were used instead of 4 ml. No difference was seen with the increased amounts compared with the 4 ml amount, and extractions continued with the 4ml amount as per protocol. The time involving the steps where Buffers P1, P2 and P3 were added was monitored carefully. As a lot of chromosomal DNA was still seen after electrophoresis (Figure 16), the lysis step involving Buffer P2 was shortened to 4 minutes in order to prevent chromosomal

DNA from being lysed, but it made no difference. The kit extraction was compared with a manual extraction. The latter resulted in a low yield with lots of contamination. p82H was extracted alongside another control BAC that was known to work in our laboratory with the Qiagen kit. The extractions were comparable.

Labelling by nick translation

Different DNase I dilutions were tried. All were diluted in 1 ml sterile water. They were 0.8 µl, 1.0µl, 1.6 µl, 1.9 µl, 2.0 µl, 2.1 µl, 2.5 µl, 3.0 µl, 4.0 µl, 5.0 µl, 5.2 µl, 5.5 µl. Only the dilution 5.5 µl in 1 ml, digested the DNA to the correct size (Figure 17). The digestion often had to be redigested for 40 minutes with another 1 µl of the DNase I dilution added to the reaction. Different DNA polymerase amounts were used, 3 µl, 4.5 µl, or 6 µl, to ensure the SpectrumOrange was being added. However, no difference was seen between them. p82H was labelled alongside another BAC that was known to work in our laboratory. Both p82H and the BAC were considered successful after electrophoresis, but where the BAC probe successfully hybridised to a metaphase slide, the p82H probe did not.

4.1.2 Synthetic probe

DNA extractions

Extractions on the whole blood and buffy coat of a sample were performed using the Flexigene DNA kit (Qiagen). The yield of the DNA was compared with that achieved from the in-house phenol chloroform method, and the in-house phenol chloroform method resulted in a much greater yield. Different EL buffers were used in the in-house phenol chloroform method, EL buffer (Qiagen) and Red cell lysis buffer (Roche). The greatest yield was observed with the Red cell lysis buffer (Roche).

PCR

20 µl reactions were originally used instead of 100 µl reactions. Different annealing temperatures were tried, 45 ºC, 49 ºC, 50 ºC, 51 ºC, 52 ºC, 53 ºC, 51.8 ºC, 52.7 ºC, 55 ºC, 56 ºC, 57 ºC, 58 ºC, 59 ºC, 60 ºC, to determine whether they would improve the concentration. It was found that the original programme (see 3.5.2.2) gave the best results.

PCR purification

The BioSpin kit required two samples to be pooled in order to get a sufficient yield. Sterile water was used to dissolve the PCR product, instead of the provided elution buffer.

Different elution amounts were tried for the Roche kit. The PCR product was eluted with 50 µl only or in two steps with 50 µl each, where the second 50 µl was added to the filter tip once the first had been centrifuged through it. The greatest yield was achieved with the single 50 µl elution step.

Labelling by nick translation

The incubation time was shortened to 30 minutes, and 0.5 µl DNase I stock diluted in 1 ml sterile water digested the DNA to the correct size. When required, the reaction was redigested for 15 minutes.

4.2 FISH

The FISH methodologies needed to be optimised in order to achieve the best results, i.e. clear strong signals with little background. The pan-centromeric probes were applied to metaphase chromosomes by means of FISH, in order to test whether the probes were able to hybridise to the centromeres of all chromosomes. The p82H probe never hybridised to any centromeres on any slide, whereas the synthetic probe did hybridise successfully to all the centromeres and clear signals could be observed. Hereafter, the term pan-centromeric probe refers to the synthetic probe. The synthetic probe was comparable with the commercial STARFISH© pan-centromeric probe.

4.2.1 FISH optimisation

Various pretreatments were tried, including a RNase only pretreatment, two different RNase and pepsin pretreatments (I and II), a pepsin only pretreatment, and slides that remained untreated were used as controls, in order to lower background and optimise the FISH. To determine how long the pepsin treatment should be in RNase and pepsin pretreatment II, micronucleus slides were incubated for 5 minutes, 7.5 minutes and 10 minutes or not treated at all. The slides were stained with acridine orange, and observed under a microscope. The desired result was to have no cytoplasm, which was achieved after 5 minutes. The various pretreatments had little effect on lowering the background and were therefore abandoned.

Changes were made to the FISH protocol in order to lower background. The wash solutions, which are usually heated to 46 °C, were heated to 47 °C - 48 °C. This did lower the background, and subsequently the solutions were heated at these temperatures in this study.

4.2.2 Classic cytogenetic test

The pan-centromeric probe was hybridized to metaphase chromosomes (Figure 8). Figure 8 shows that the synthetic pan-centromeric probe hybridized to the centromeres of all 46 chromosomes, indicating successful probe preparation and labelling. Another metaphase slide was hybridised with the commercial STARFISH© pan-centromeric probe. The two probes were comparable with one another, both in hybridising to all of the chromosomes and in signal strength.

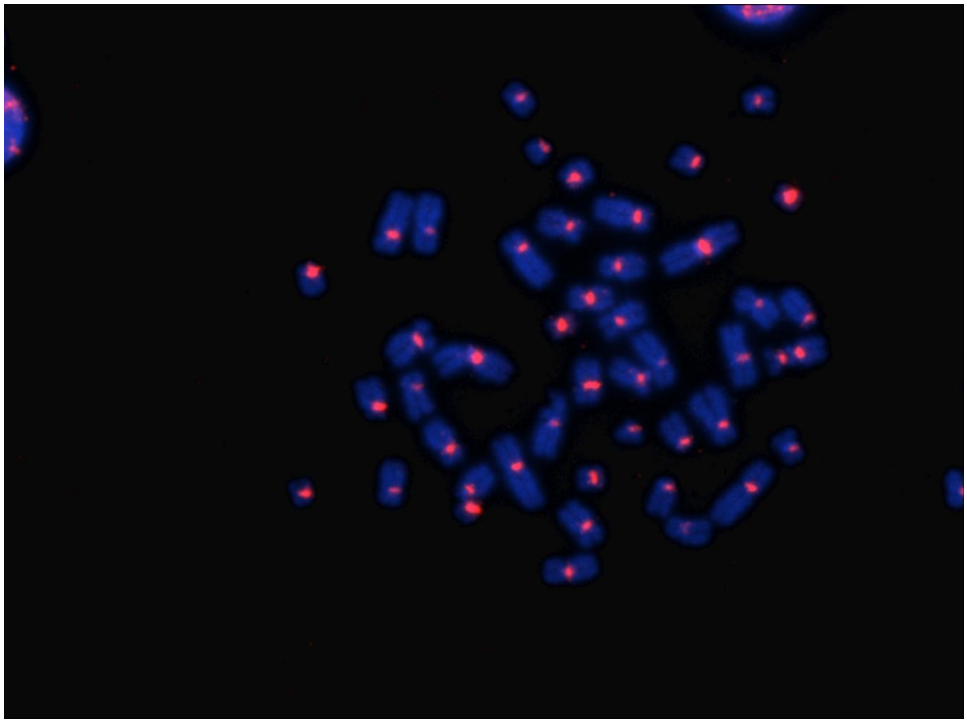

Figure 8: DAPI stained metaphase chromosomes (blue) showing the synthetic pan-centromeric probe (red signals) hybridising to all 46 chromosomes

4.2.3 Micronucleus assay

The pan-centromeric probe was hybridized to micronucleus slide preparations (Figure 9). Figure 9A shows a binucleated cell with a single micronucleus containing 3 signals. This indicates that the micronucleus was centromere-positive, and assumed to be a result of aneugenic events i.e. the loss of whole chromosomes due to chromosome lagging etc. The signal may be a separate chromosome or chromatid expelled from the cell. In this study, the centromere-positive cells were considered to be a result of spontaneous damage. Figure 9B shows a binucleated cell with a single micronucleus without any signals. The pan-centromeric probe hybridised to the centromeres in the main nuclei therefore the lack of signal was not because of poor hybridisation. Centromere-negative cells arise as a result of clastogenic events, where chromosomal fragments are lost from the cell due to the action of a clastogen, in this case, radiation.

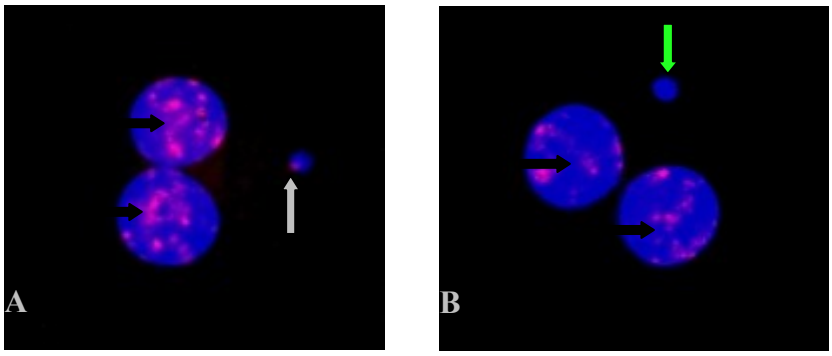

Figure 9: DAPI stained binucleated cells hybridised with the pan-centromeric probe with a single micronucleus with (A) or without a signal (B). A) DAPI-stained binucleated cell with a single micronucleus exhibiting a signal (white arrow), within the micronucleus. Therefore the micronucleus is centromere-positive. B) DAPI-stained binucleated cell with a single micronucleus showing no signals (green arrow). The micronucleus is, therefore, centromeric-negative. Note that the pan-centromeric probe has bound to the centromeres within the main nuclei (black arrows) thereby acting as a control to ensure FISH was successful.

4.3 Dose-response study

All of the blood samples collected were from women, and none were smokers. The samples were also age-matched.

4.3.1 Automated versus semi-automated scoring

Scoring completely automatically was compared with scoring semi-automatically with the Wilcoxon signed rank test. The results of this comparison are shown in Figure 10, with the standard deviation. A significant difference ($p < 0.05$) was found between the two. Note, also, that the semi-automated scoring follows a linear quadratic form, whereas the automated scoring does not in the area of the low doses (0 Gy – 0.5 Gy). The slides were scored under a single filter, i.e. DAPI, where the automated scoring includes everything that the MetaFer scored as a binucleated cell containing micronuclei, and the semi-automated scoring includes only true binucleated cells with true micronuclei, false positives were excluded by the scorer. Consequently, scoring was performed semi-automatically for further studies.

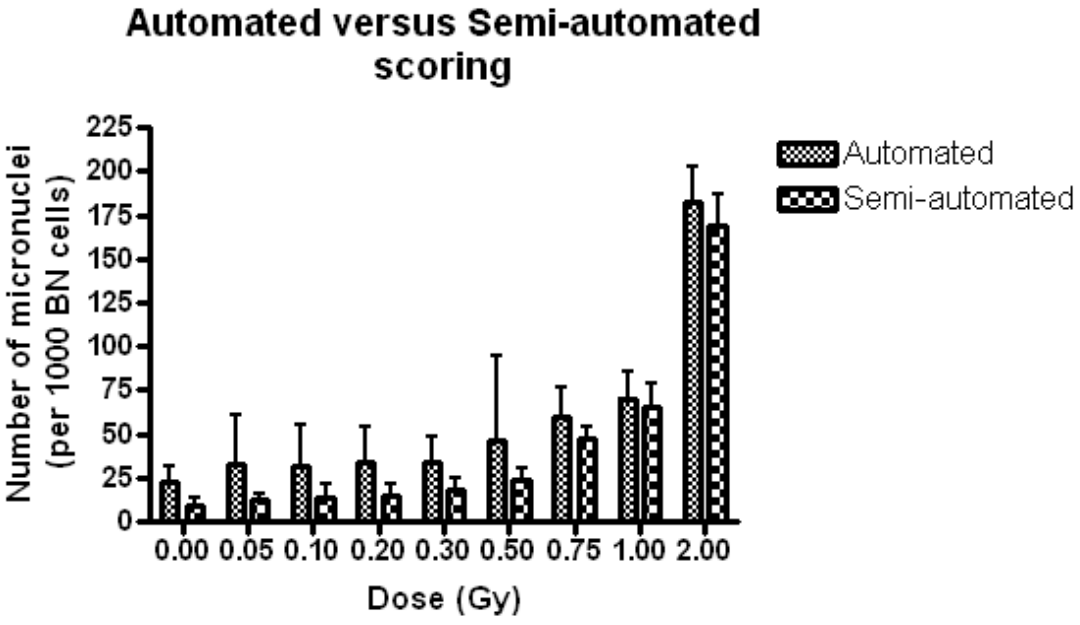

Figure 10: The total number of micronuclei scored completely automatically or semi-automatically (standard deviation indicated by error bars).

4.3.2 Dose response curves

The samples were scored for micronuclei on the automated MetaFer system semi-automatically with a dual filter (DAPI and SpectrumOrange). The total number of micronuclei scored semi-automatically is plotted in Figure 11, with Figure 11A showing all doses and Figure 11B showing the low doses. Figure 12 shows these micronuclei classified as centromere-positive or centromere-negative based on whether or not a pan-centromeric signal was present. The percentage of centromere-negative micronuclei was plotted in Figure 13. The dose response curves are linear quadratic curves.

A

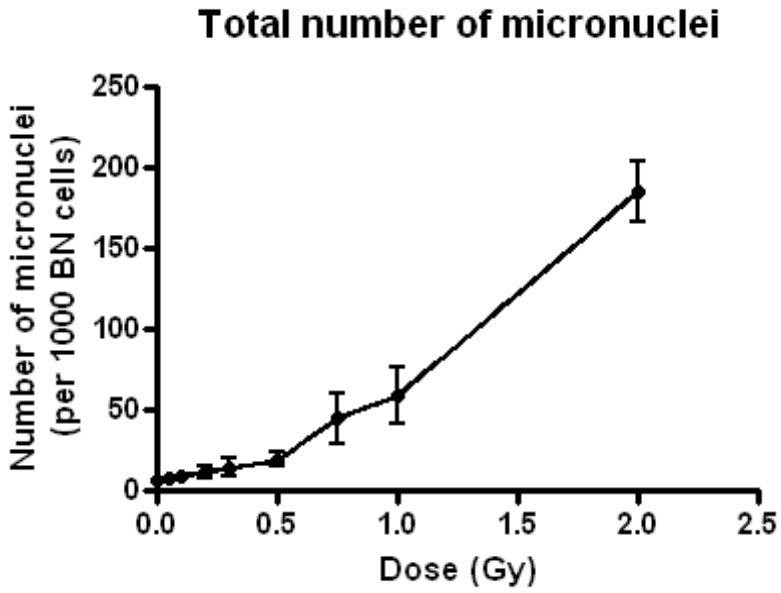

B

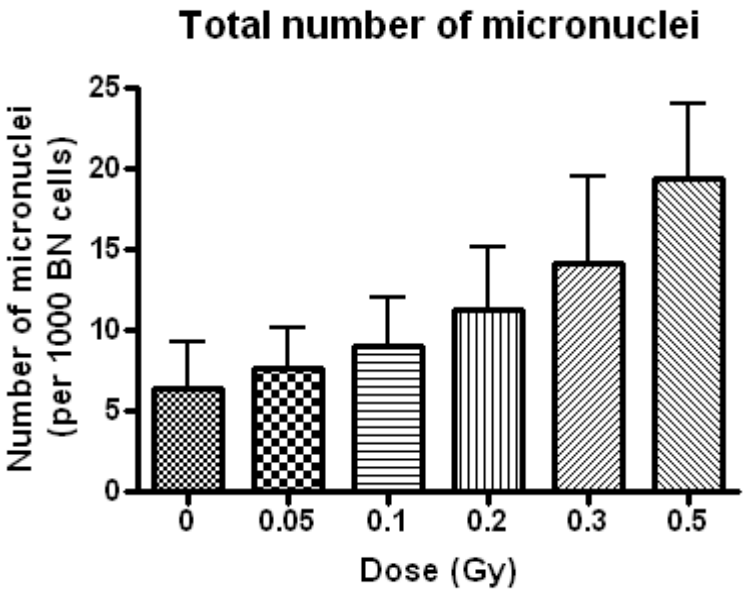

Figure 11: The averages of total number of micronuclei scored, arising as a result of exposure to different doses of gamma radiation (standard deviation indicated by error bars). Figure 11A shows results for doses 0 Gy to 2 Gy, while Figure 11B shows results for the low doses (0 Gy to 0.5 Gy).

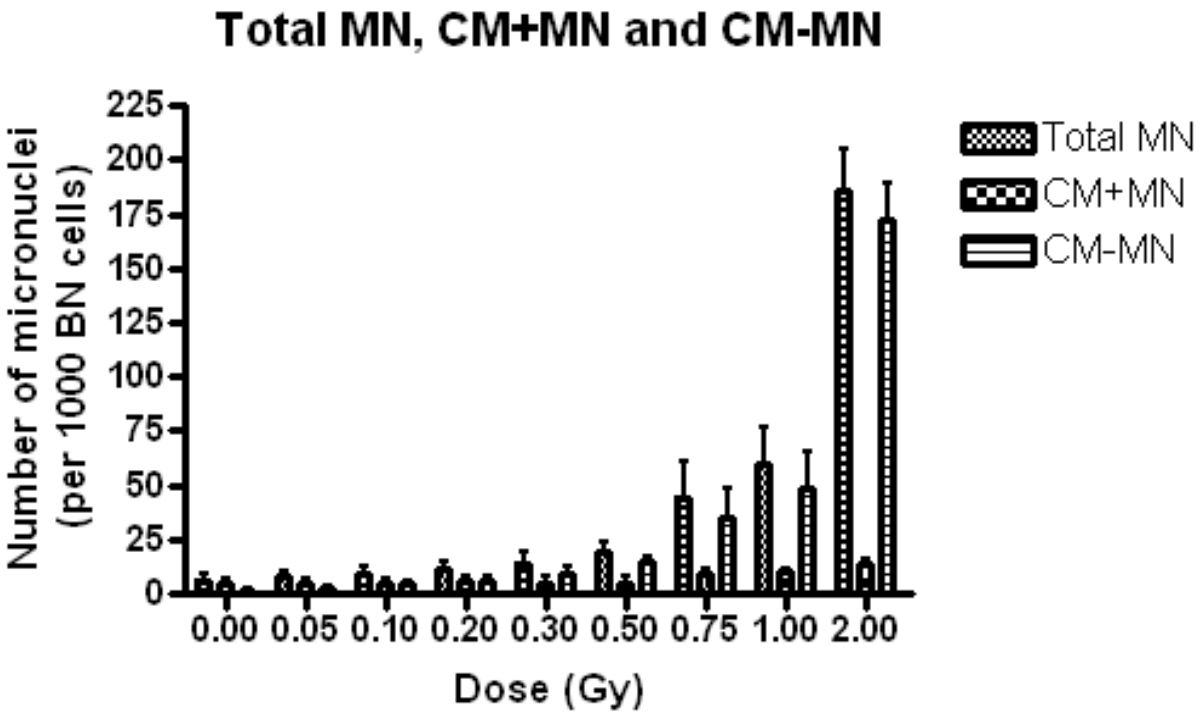

A

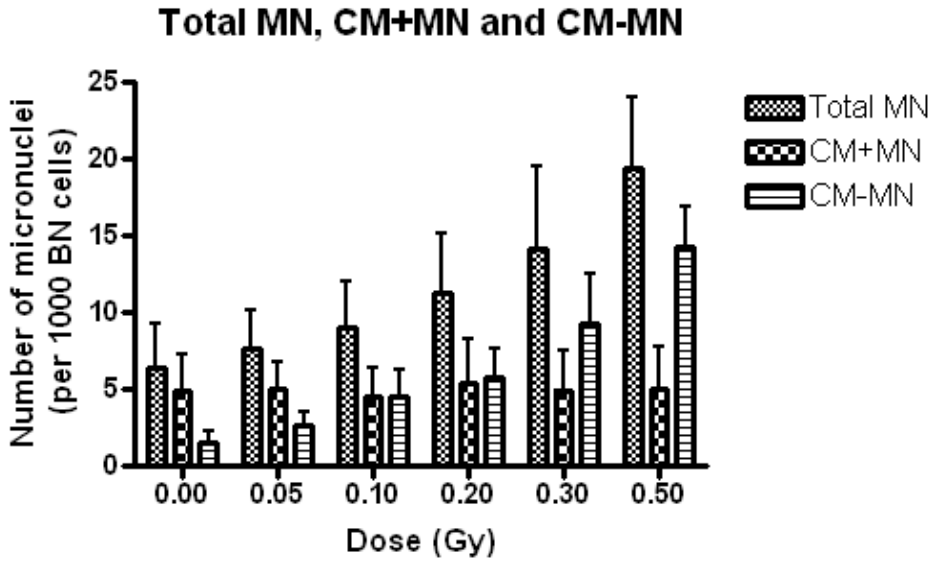

B

Figure 12: The averages of total micronuclei (Total MN), centromere-positive micronuclei (CM+MN) and centromere-negative micronuclei (CM-MN) at all doses (Figure 12A) and at low doses (Figure 12B). Standard deviation indicated by error bars.

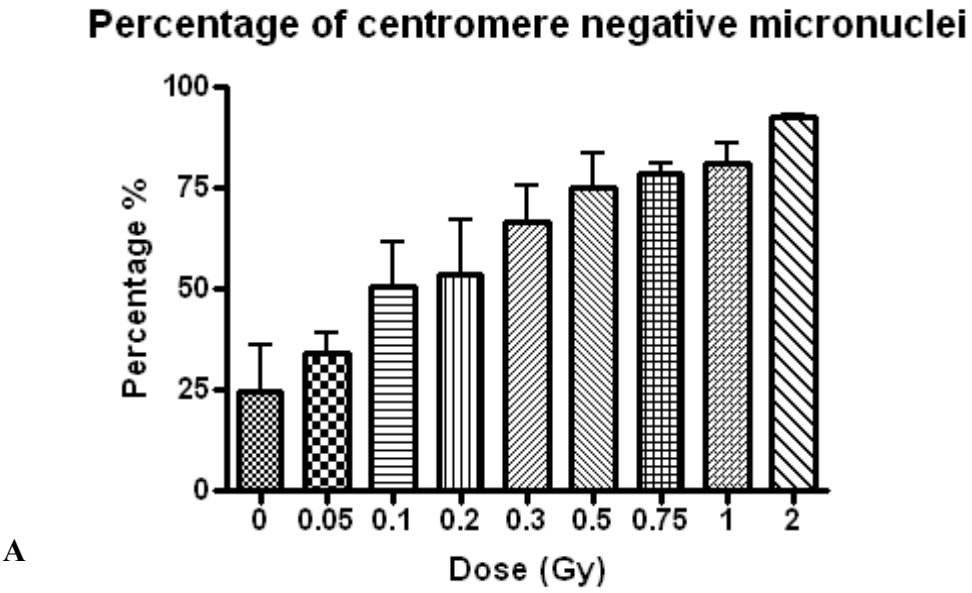

A

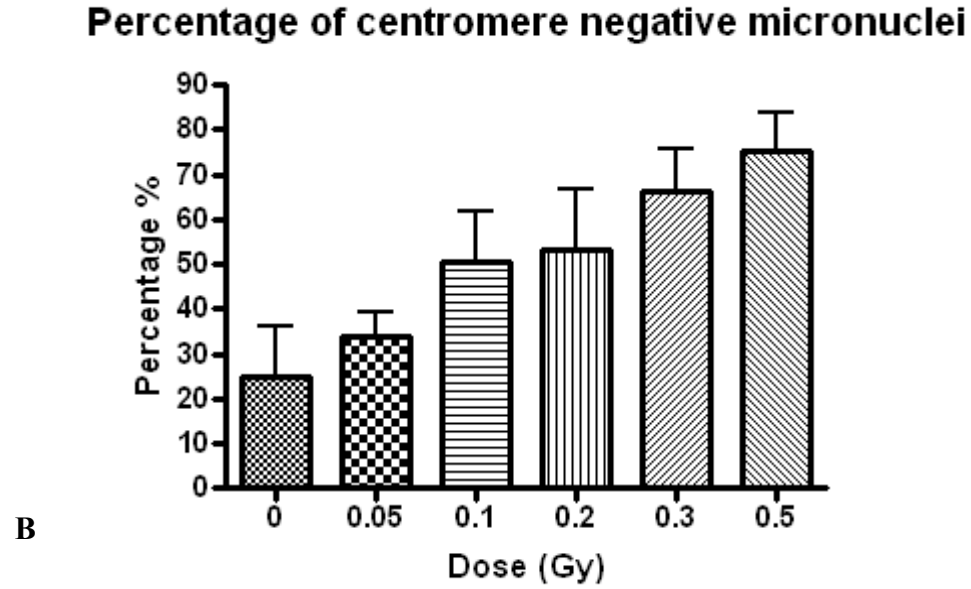

B

Figure 13: The percentages of centromere-negative micronuclei scored at different doses of gamma radiation (standard deviation indicated by the error bars). Figure 13A shows results for the doses, 0 Gy to 2 Gy, and Figure 13B shows results for the low doses (0 Gy to 0.5 Gy).

Table 4: Significant differences in the total number of micronuclei and the percentage of centromere-negative micronuclei between doses using the Wilcoxon signed rank test

Dose (Gy)	Significant difference in micronucleus counts (95 % Confidence Intervals)	Significant difference in percentage centromere-negative micronuclei (95 % Confidence Intervals)
0 – 0.05	* (p = 0.0488)	* (p = 0.0273)
0.05 – 0.1	×	* (p = 0.0020)
0.1 – 0.2	* (p = 0.0059)	×
0.2 – 0.3	×	* (p = 0.0039)
0.3 – 0.5	* (p = 0.0020)	* (p = 0.0137)
0.5 – 0.75	×	×
0.75 – 1	×	×
1 – 2	×	×

* indicates a statistically significant difference was found between the doses.

× indicates no statistically significant difference was found.

The pan-centromeric marker combined with the micronucleus assay can accurately differentiate between spontaneous (CM+MN) and radiation-induced micronuclei (CM-MN). Significant differences were observed (Table 4) based on total micronucleus counts and percentage of CM-MN between low doses, which confirms previous work (Pala et al, 2008; Vral et al, 1997); significant differences were observed with a dose as low as 0.05 Gy, which has not been previously reported.

4.4 HIV study

The HIV+ samples and controls were age-matched and sex-matched, the majority were women and non-smokers. The first part of the HIV study involved micronucleus assays performed on blood samples collected from 19 HIV+ patients and 13 HIV- controls. The blood cultures were exposed to 2 Gy and 4 Gy doses of X-irradiation, and control blood cultures were mock-irradiated. These samples were scored manually for micronuclei, as shown in Figure 14. The data collected was analysed using the Mann-Whitney Test with confidence intervals set at 95 %. A p-value > 0.05 was found, therefore no significant difference was observed between the HIV+ and HIV- samples at any dose.

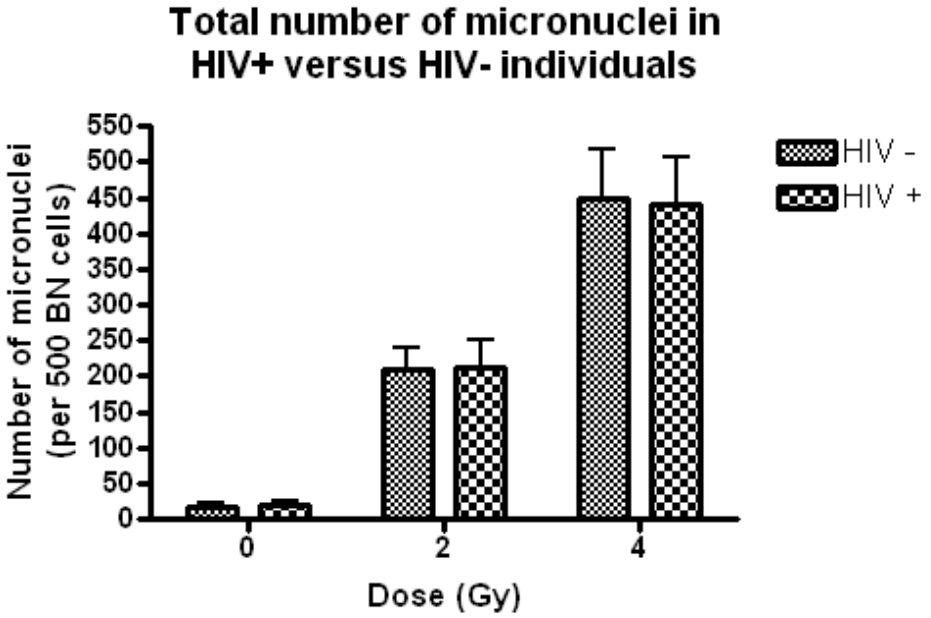

Figure 14: The average number of total micronuclei of HIV+ versus that of HIV- samples exposed to doses of 0 Gy, 2 Gy and 4 Gy X-radiation (standard deviation indicated by error bars).

In the second part of the HIV study, eight HIV+ and four HIV- samples were not irradiated and were analysed semi-automatically on the MetaFer system. This was done because no significant differences were found between the total micronucleus counts of HIV+ and HIV- samples (Figure 14) according to the Mann-Whitney test ($p > 0.05$), and these results were unexpected, as data collected in a previous study indicated a significant difference between HIV+ and HIV- chromosomal sensitivity (Baeyens et al, 2010). The slides from the unexposed samples were hybridised with the pan-centromeric probe (Figure 15) and were scored semi-automatically on the MetaFer, and analysed with the Mann-Whitney test. Although there are no significant differences in the total number of micronuclei found between HIV+ and HIV- individuals, a slightly higher number of total micronuclei in the HIV+ individuals was noticed, which was attributed to the number of CM+MN.

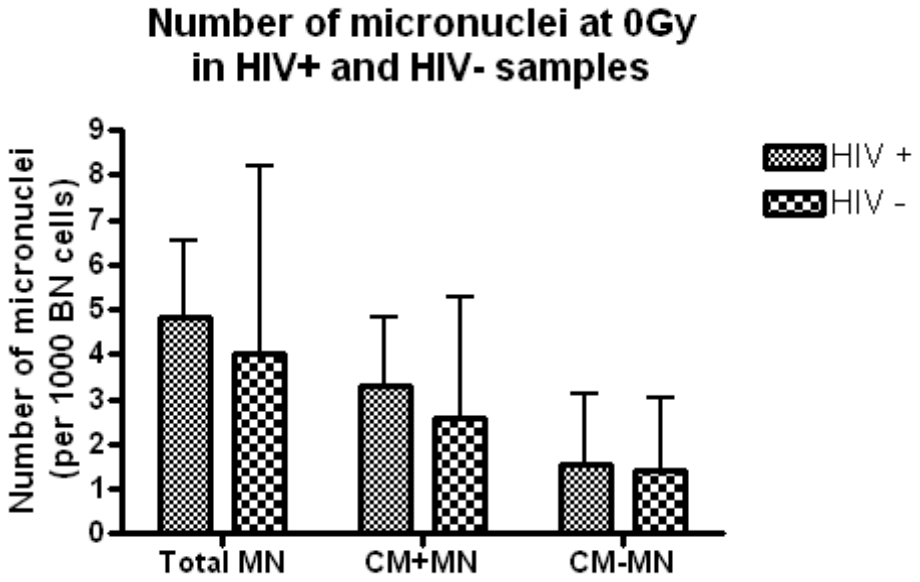

Figure 15: The number of total micronuclei (Total MN), centromere-positive (CM+MN) and centromere-negative micronuclei (CM-MN), from unexposed HIV+ and HIV- samples (standard deviation indicated by error bars).

CHAPTER FIVE – DISCUSSION

This study aimed to develop a pan-centromeric probe, and optimise it for use in cases of radiation exposure, and possibly for routine biomonitoring of radiation workers. In order to accomplish this, two different methods for the preparation of the pan-centromeric probe were tried, the p82H probe and the synthetic pan-centromeric probe. The probe was applied to cells that were exposed to various doses of gamma radiation, and the damage was examined. From the amount of micronuclei, dose response curves could be set up. Lastly, the chromosomal radiosensitivity of HIV-infected individuals was explored.

Only the synthetic pan-centromeric probe successfully labelled the centromeres. The plasmid, p82H, was successfully extracted (Figure 16, Appendix B) and labelled by means of nick translation (Figure 17, Appendix B), but failed to bind to the centromeres of any chromosome. It was speculated that the plasmid had lost the p82H insert. The synthetic probe was isolated from extracted human male DNA through PCR with specified primers (Figure 18, Appendix B), and labelled by means of nick translation (Figure 19, Appendix B). A possible improvement to this method may be to label the synthetic probe during PCR. Backx et al (2008) showed that labelling Bacterial Artificial Chromosomes (BAC) clones during Degenerative Oligonucleotide Primed (DOP)-PCR resulted in strong FISH signals with minimal background as compared with the clones that were labelled by means of traditional methods. The thermobrite (Abbott Molecular), is a machine, which uses temperature to denature the DNA and hybridise the probe to a slide. It would reduce time by eliminating the denaturing step of the manual FISH procedure.

For the dose response study, the samples were exposed to gamma radiation from a Cobalt-60 source. Gamma radiation is highly energetic and a highly

penetrative form of electromagnetic radiation. It is often used as a standard in radiation studies, and other radiation types are compared with it. X-radiation was used in the HIV study. It is also a highly energetic and penetrative form of radiation, and is very similar to gamma radiation.

The micronucleus assay is a valuable, thoroughly validated and standardised technique that can be used to evaluate radiation exposure of occupationally, medically and accidentally exposed individuals, and to assess in vitro radiosensitivity. The scoring of micronuclei is simple, quick and does not require specific experience in cytogenetics. No special equipment is needed and the cost is low. However, one drawback is that it is not sensitive enough to distinguish between exposures to low doses of ionising radiation. The restricted sensitivity of the micronucleus assay is because of the relative high and variable spontaneous micronucleus yield. The most important factors influencing this background are age and sex (Fenech et al, 1994; Thierens et al, 1996). Detection of centromeres showed that the age increase of background micronuclei can be attributed almost totally to centromere-positive micronuclei, reflecting an increased chromosome loss with age. This restricted sensitivity is a problem as most exposures occur at low doses. Combining the micronucleus assay with FISH using a pan-centromeric probe greatly enhances the sensitivity of the test allowing the distinction of and between ionising radiation doses, especially important among the very low dose range (0.05 Gy, 0.1 Gy, 0.2 Gy). The pan-centromeric probe allowed the distinction between centromere-positive (spontaneous) micronuclei, and centromere-negative micronuclei, which arose as a result of exposure to damaging agents, in this case ionising radiation. Several studies have validated (Wojcik et al, 2000) and used the micronucleus-centromere assay in cytogenetic studies and biomonitoring projects (Thierens et al, 1999; Sari-Minodier et al, 2002; Bolognesi et al, 2004) that involved radiation or exposure to other clastogenic agents. These

studies found that the micronucleus-centromere assay was more sensitive than the normal micronucleus assay, and that the total micronucleus frequency was higher in exposed groups and the amount of centromere-negative micronuclei was also higher in exposed groups.

The results of the study corroborate those found previously by Vral et al (1997), where the damages induced, i.e. amount of micronuclei, and among these, the amount of centromere-negative micronuclei, by the same doses are similar. In this study, a statistically significant difference could be seen with a dose as low as 0.05 Gy compared with the unirradiated sample both in the micronuclei count and in the percentage increase of centromere-negative micronuclei. The percentage of centromere-negative micronuclei, which may arise because of exposure to ionising radiation, can therefore help with evaluating the initial exposure dose. This is important when no significant difference is found between the total micronuclei counts of different doses, as in the case between 0.05 Gy and 0.1 Gy, where a statistically significant difference could be seen in the percentage of centromere-negative micronuclei. Similarly this was observed between 0.2 Gy and 0.3 Gy. Future studies may focus on investigating whether the test could be used in extremely low dose exposures, i.e. doses below 0.05 Gy. The dose-response curve, therefore, showed that the micronucleus-centromere assay adds a significant improvement for an effective biomonitoring methodology.

Although the LNT model is followed, some studies have indicated that low doses of radiation can be beneficial, as is the case of the adaptive response in radiation, which showed that exposure to a low dose of radiation could partially protect against a larger dose (Wolff, 1998). It was hypothesised that the low dose exposure activated a repair mechanism, which was active when the larger dose was applied, and could repair some of the damage induced.

However, this adaptive response depended on several factors, such as a minimal dose before it can become active, dose rate, individual radiosensitivity, and the magnitude of the dose. Newer work has explored the presence and/or lack of mRNAs, and changes in gene transcription that resulted from irradiation (Wolff, 1998).

The automation of the micronucleus-centromere assay greatly improves the test for use over manual scoring (Schunck et al, 2004, Varga et al, 2004; Willems et al, 2010). It reduces the turnover time of the test, allows for high-throughput, which is important with regards to large radiation accidents or for biomonitoring projects where large populations need to be tested.

There is a great variation regarding chromosomal radiosensitivity, which is affected by smoking habits, age (increases with age), gender (females have greater radiosensitivity), and even physiological conditions (such as pregnancy) (Bonassi et al, 2003; Fenech et al, 1994; Fenech, 1998; Ricoul et al, 1997; Thierens et al, 1996). It has been observed clinically and in previous published data that HIV+ individuals exhibit a greater radiosensitivity to ionising radiation than uninfected individuals, and that this difference is statistically significant (Baeyens et al, 2010). This raises a few concerns regarding the treatment for cancer patients that are HIV+, and the protection of HIV+ radiation workers. It is, therefore, important to explore this further to ensure optimal treatment and sufficient protection.

The regulations regarding radiation protection do not completely take into account an individual's response to radiation, and their variation in radiosensitivity. Low doses that are considered “safe” by protection standards may not be so in an individual, if they are unable to detect or repair the damage. These individuals would be at increased risk in any

environment involving radiation. Schnarr et al (2007) found large variation between individuals and in different cellular populations. They found that the largest variation was observed in the CD4+ T-cell sub-population compared with CD8+ T-cell and total lymphocyte populations. Moreover, they also found that with increasing age, the lymphocytes became less sensitive to radiation.

Different sub-populations of T-cells have different susceptibilities to ionising radiation. Wilkins et al (2002) explored this in their study when they isolated different sub-populations of white blood cells and exposed the isolated sub-populations to low doses of X-rays. They observed that CD4+ T-cells and CD8+ T-cells were the most radiosensitive, and CD8+ T-cells were more sensitive than CD4+ T-cells based on their apoptotic fractions. Co60-radiation has been shown to induce more micronuclei in CD4+ T-cells, compared with CD8+ T-cells (Holmen et al, 1994), but other types of radiation have been shown to induce more micronuclei in CD8+ T-cells (Wuttke et al, 1993). Both studies used the same assay. CD4+ T-cells were found by Stern et al (1994) to have a greater sensitivity to the genotoxic effects of the antiretroviral (ARV) drug, 3-azido-3-deoxythymidine (AZT) compared with CD8+ T-cells. In their review, Weng and Morimoto (2009), noted that CD4+ T-cells appeared to be less sensitive than CD8+ T-cells when activated, but more sensitive when not activated, and that CD4+ T-cells have higher micronuclei counts in response to mutagens as compared with CD8+ T-cells. It has also been observed that HIV+ patients display compromised normal tissue tolerance during radiotherapy. Data collected from HIV+ patients and uninfected controls shows that micronucleus frequencies are consistently higher in HIV+ patients (Baeyens et al, 2010).

Despite previous published data (Baeyens et al, 2010), this study has found no significant differences between HIV+ individuals and an uninfected

group (Figure 14). Many samples had to be excluded because too few cells were obtained for accurate analysis. The previous published data where HIV+ were more radiosensitive than HIV- individuals did raise the question whether this higher sensitivity to radiation is caused by chromosomal instability. A higher chromosomal instability would result in a higher CM+MN count, which was seen in this study.

There are certain difficulties in applying the micronucleus assay to HIV infected people, already low CD4 counts below 200 cells/mm^3 were excluded from the study as previous data found too few cells for appropriate analysis, and infected people treated with HAART were also excluded as the treatments might have interfered with the results of the assay. The HIV infected samples produced fewer viable cells in the assay resulting in lower yields compared with uninfected controls. This poor proliferative response has been observed previously, as well as cell death after lymphocyte stimulation, in HIV+ populations. Medina et al (1994) noted that no matter what mitogen was used to stimulate the lymphocytes to divide, a number of the lymphocytes from the HIV+ sample died prematurely. It was also noted that stronger mitogens, such as PHA, exert a greater effect i.e. more cells die prematurely, which may be because lymphocytes respond faster to PHA. They attributed this loss to Activation-Associated Lymphocyte Death (AALD). It was observed that AALD affected the different sub-populations differently. In general, it occurred in CD8+ T-cells more than CD4+ T-cells, but it was found it occurred in greatest frequency in memory CD4+ T-cells of HIV+ individuals in their study (Medina et al, 1994). Furthermore, a large variation among individuals CD4+ T-cells sub-populations was found (Schnarr et al, 2007).

HIV was previously reported to be relatively resistant to X-irradiation (Henderson et al, 1992), and its reverse transcriptase has the ability to read

through damaged bases. But this study was performed on the virus alone and not in infected cells. In HIV infected cells, Sun et al (2006) found that radiosensitivity increased in Tat-expressing cells and that the cells were unable to repair many radiation-induced DNA DSBs. Many cycle-related genes, such as *DNA-PK$_{CS}$*, *Cdc20,Cdc25C, KIF2C, CTS1*, were also down-regulated. They suggested that HIV Tat was responsible for the enhanced radiosensitivity, because it hindered repair and cell-cycle checkpoints. HIV Tat does impair telomerase in infected lymphocytes (Franzese et al, 2004), and it is involved in gene expression (Freed, 2001)

Accessory HIV proteins, like Viral Protein R (Vpr), may also play a role. Vpr has a number of effects on the infected cell and is involved in many processes, including reverse transcription, nuclear import, cell cycle progression, regulation of apoptosis, gene expression (Le Rouzic and Benichou, 2005). Vpr recruits a DNA repair enzyme, UNG, to the virus particle. It can induce cell-cycle arrest at the G2 phase, just before integration of the viral DNA, and is capable of inducing apoptosis by acting on the mitochondria. This Vpr-mediated arrest is different from one caused by DNA damage, and allows optimal conditions for the HIV transcription. Vpr up- or down-regulates various cell genes. Vpr can rupture the nuclear envelope, which may cause DNA damage such as DSBs. It has a high affinity for nucleic acids (Le Rouzic and Benichou, 2005). Overexpression of Vpr has been observed with abnormalities in mitosis, cytokinesis and nuclear structure (Skalka and Katz, 2005). Vpr has also been implicated in micronucleus formation and aneuploidy (Shimura et al, 1999a; Shimura et al, 1999b)

The integration process, whereby the virus inserts its DNA into the host genome, results in a complex lesion. The lesion interrupts the chromatin conformation and composition. The damage is repaired by specific

pathways, but some may escape and lead to DSBs. The infected cells repair the damage as they would for radiation-induced DSBs because of the chromatin alteration, the free DNA ends and the integration intermediates, which resemble the damage repaired by NHEJ (Skalka and Katz, 2005). The PIC contains various proteins, which may be involved in chromatin remodelling (Freed, 2004). The chromatin remodelling may leave the DNA more open, and therefore more susceptible to damage from ionising radiation.

A pan-centromeric probe was developed and optimised for use in the micronucleus assay combined with FISH. This assay can be automated on the MetaFer system successfully, making the assay faster and adaptable for large-scale studies. The dose response study allowed the detection of doses of ionising radiation as low as 0.05 Gy, and the pan-centromeric probe showed that even among doses where the total micronucleus counts were not significantly different, it was still possible to distinguish between doses based on their percentage of centromere-negative micronuclei. This study did not show any significant difference between HIV+ individuals and uninfected individuals, but showed a higher chromosomal instability in HIV+ individuals. Little is understood as to why HIV+ samples exhibit enhanced radiosensitivity. The micronucleus assay coupled with FISH using a pan-centromeric probe proved to be a sensitive tool in this study. It was adapted to an automated system, and very low doses of ionising radiation could be detected. It could make an effective tool for biomonitoring, and greatly aid future studies.

CHAPTER SIX – CONCLUSIONS

- The micronucleus assay combined with a pan-centromeric probe greatly enhances the sensitivity of the test allowing the distinction of and between ionising radiation doses.
- The micronucleus-centromere assay can be automated, allowing high-throughput, which is important regarding large-scale radiation accidents and biomonitoring projects.
- HIV+ samples were not found to be more radiosensitive than HIV- samples in this study, contrary to previous published data.
- A higher CM+MN count was observed in the HIV+ samples, which suggests a higher chromosomal instability among HIV+ people.

REFERENCES

The AIDS 2008 Impact Report. XVII International AIDS Conference.

Aleixandre C, Miller DA, Mitchell AR, Warburton DA, Gersen SL, Disteche C, Miller OJ. 1987. p82H identifies sequences at every human centromere. Hum. Genet. **77**: 46–50.

Angerer J, Ewers U, Wilhelm M. 2007. Human biomonitoring: State of the art. International Journal of Hygiene and Environmental Health, 210: 201–228.

Au WW. 2007. Usefulness of biomarkers in population studies: From exposure to susceptibility and to prediction of cancer. International Journal of Hygiene and Environmental Health, 210: 239–246.

Aukrust P, Luna L, Ueland T, Johansen RF, Muller F, Froland SS, Seeberg EC, Bjoras M. 2005. Impaired base excision repair and accumulation of oxidative base lesions in CD4+ T cells of HIV infected patients. Blood 105: 4730–4735.

Backx L, Thoelen R, Van Esch H, Vermeesch JR. 2008. Direct fluorescent labelling of clones by DOP PCR. Molecular Cytogenetics 1: 3.

Baeyens A. 2005. *In Vitro* Chromosomal Radiosensitivity in Breast Cancer Patients. PHD thesis.

Baeyens A, Slabbert JP, Willem P, Vral A. 2007. Radiosensitivity of Lymphocytes in HIV Positive Individuals. SAAPMB Congress.

Baeyens A, Slabbert JP, Willem P, Jozela S, van der Merwe D, Vral A. 2010. Chromosomal radiosensitivity of HIV positive individuals. International Journal of Radiation Biology. In publication.

Bolognesi C, Landini E, Perrone E, Roggieri. 2004. Cytogenetic biomonitoring of a floriculturist population in Italy: micronucleus analysis by fluorescence in situ hybridisation (FISH) with an all-chromosome centromeric probe. Mutation Research 557: 109–117.

Bonassi S, Neri M, Lando C, Ceppi M, Lin Y-P, Chang WP, Holland N, Kirsch-Volders M, Zeiger E, Fenech M. 2003. Effect of smoking habit on the frequency of micronuclei in human lymphocytes: results from the Human MicroNucleus project. Mutation Research 543: 155–166.

Campbell EM, Hope TJ. 2008. Live cell imaging of the HIV-1 life cycle. Trends in Microbiology 16: 580–587.

Christmann M, Tomicic MT, Roos WP, Kaina B. 2003. Mechanisms of human DNA repair: an update. Toxicology 193: 3–34.

Darroudi F, Fomina J, Meijers M. 2008. Biological Dosimetry in cases of accidental and occupational exposure to ionising radiation: State of the art. Radioprotection, 43: 27–31.

Dianiak N, Waselenko JK, Armitage JO, MacVittie TJ, Farese AM. 2003. The Hematologist and Radiation Casualties. Hematology 473–496.

Fenech M, Morley AA. 1985. Measurement of micronuclei in human lymphocytes. Mutat. Res. 148: 29–36.

Fenech M, Neville S, Rinaldi J. 1994. Sex is an important variable affecting spontaneous micronucleus frequency in cytokinesis-blocked lymphocytes. Mutation Research 313: 203–207.

Fenech M. 1998. Important variables that influence base-line micronucleus frequency in cytokinesis-blocked lymphocytes – a biomarker for DNA damage in human populations. Mutation Research 404: 155–165.

Fenech, M. 2000. The *in vitro* micronucleus technique. Mutation Research 455: 81–95.

Franzese O, Comandini A, Adamo R, Sgadari C, Ensoli B, Bonmassar E. 2004. HIV-Tat down-regulates telomerase activity in the nucleus of human CD4+ T cells. Cell Death and Differentiation 11: 782–784.

Freed EO. 1998. HIV-1 Gag proteins: diverse functions in the virus life-cycle. Virology 251: 1–15.

Freed EO. 2001. HIV-1 Replication. Somatic Cell and Molecular Genetics 26: 13–33.

Freed EO. 2004. HIV-1 and the host cell: an intimate association. TRENDS in Microbiology 12: 170–177.

Galati D, Bocchino M, Paiardini M, Cervasi B, Silvestri G, Piedimonte G. 2002. Cell Cycle Dysregulation During HIV Infection: Perspectives of a Target Based Therapy. Current Drug Targets – Immune, Endocrine & Metabolic Disorders 2: 53–62.

Henderson EE, Tudor G, Yang J-Y. 1992. Inactivation of the Human Immunodeficiency Virus Type 1 (HIV-1) by Ultraviolet and X Irradiation. Radiation Research 131: 169–176.

Hittelman WN, Pandita TK. 1994. Possible role of chromatin alteration in radiosensitivity of Ataxia Telangiectasia . Int. J. Radiat. Biol., **66**: 109–113.

Hoeijmakers JHJ. 2001. Genome maintenance mechanisms for preventing cancer. Nature, **411**: 366–374.

Holmen A, Karlsson A, Bratt I, Hogstedt B. 1994. Micronuclei and mitotic index in B-, T4- and T8-cells treated with mitomycin-C and γ-irradiation. Mutation Research, 309: 93–99.

Iarmarcovai G, Botta A, Orsièse T. 2006. Number of centromeric signals in micronuclei and mechanisms of aneuploidy. Toxicology Letters **166**: 1–10.

Jeeninga RE, Westerhout EM, van Gerven ML, Berkhout B. 2008. HIV-1 latency in actively dividing human T-cell lines. Retrovirology 5: 37

Kanaar R, Hoeijmakers JHJ, Van Gent DC. 1998. Molecular mechanisms of DNA double-strand break repair. Trends Cell Biol., 8: 483–489.

Khanna KK, Jackson SP. 2001. DNA double-strand breaks: signalling, repair and the cancer connection. Nat. Genet., **27**: 247–254.

Le Rouzic E, Benichou S. 2005. The Vpr protein from HIV-1: distinct roles along the viral life cycle. Retrovirology 2:11

Lindberg HK, Wang X, Järventaus H, Falck GCM, Norppa H, Fenech M. 2007. Origin of nuclear buds and micronuclei in normal and folate-deprived human lymphocytes. Mutation Research **617**: 33–45.

Little JB, Nagasawa H. 1985. Effect of confluent holding on potentially lethal damage repair, cell cycle progression and chromosome aberrations in human normal and Ataxia Telangiectasia fibroblasts. Radiat. Res., **101**: 81–93.

Ma Y, Pannicke U, Schwarz K, Lieber MR. 2002. Hairpin Opening and Overhang Processing by an Artemis/DNA-Dependent Protein Kinase Complex in Nonhomologous End Joining and V(D)J Recombination. Cell 108: 781–794.

Medina E, Borthwick N, Johnson MA, Miller S, Bofill M. 1994. Flow cytometric analysis of the stimulatory response of T cell subsets from normal and HIV-1^{+} individuals to various mitogenic stimuli in vitro. Clin. Exp. Immunol. 97: 266–272.

MetaFer manual. 2005. MetaSystems. MSearch manual V.3.1: 9 – 11.

Mitchell AR, Gosden JR, Miller DA. 1985. A cloned sequence, p82H, of the alphoid repeated DNA family found at the centromeres of all human chromosomes. Chromosoma **92**: 369–377.

Pala FS, Alkaya F, Tabakcioglu K, Tokatli F, Uzal C, Parlar S, Algunes C. 2008. The effects of micronuclei with whole chromosome on biological dose estimation. Turk. J. Biol. 32: 283–290.

Parshad R, Sanford KK, Jones GM. 1983. Chromatid damage after G2 phase x-irradiation of cells from cancer prone individuals implicates deficiency in DNA repair. Proc. Natl. Acad. Sci. USA, **80**: 5612–5616.

Pfeiffer P, Goedecke W, Kuhfittig-Kulle S, Obe G. 2004. Pathways of DNA double-strand break repair and their impact on the prevention and formation of chromosomal aberrations. Cytogenet. Genome Res 104: 7–13.

Preston RJ. 1980. DNA repair and chromosome aberrations: the effect of cytosine arabinoside on the frequency of chromosome aberrations induced by radiation and chemicals. Teratog. Carcinog. Mutagen, **1**: 147–159.

Ricoul M, Sabatier L, Dutrillaux B. 1997. Increased chromosome radiosensitivity during pregnancy. Mutation Research – Fundamental and Molecular Mechanisms of Mutagenesis 374: 73–78.

Rothkamm K, Lobrich M. 2003. Evidence for a lack of DNA double-strand break repair in human cells exposed to very low x-ray doses. PNAS 100: 5057–5062.

Sanford KK, Parshad R, Gantt R, Tarone RE, Jones GM, Price FM. 1989. Factors affecting and significance of G2 chromatin radiosensitivity in predisposition to cancer. Int. J. Radiat. Biol., **55**: 963–981.

Sari-Minodier I, Orsiere T, Bellon L, Pompili J, Sapin C, Botta A. 2002. Cytogenetic monitoring of industrial radiographers using the micronucleus assay. Mutation Research 521: 37–46.

Schnarr K, Dayes I, Sathya J, Boreham D. 2007. Individual radiosensitivity and its relevance to health physics. Dose-Response 5: 333–348.

Schunck C, Johannes T, Varga D, Lorch T, Plesch A. 2004. New developments in automated cytogenetic imaging: unattended scoring of dicentric chromosomes, micronuclei, single cell gel electrophoresis, and fluorescence signals. Cytogenetic and Genome Research, 104: 383–389.

Scott D, Barber JBP, Spreadborough AR, Burrill W, Roberts SA. 1999. Increased chromosomal radiosensitivity in breast cancer patients: a comparison of two assays. Int. J. Radiat. Biol., **75**: 1–10.

Shimura M, Tanaka Y, Nakamura S, Minemoto Y, Yamashita K, Hatake K, Takaku F, Ishizaka Y. 1999a. Micronuclei formation and aneuploidy induced by Vpr, an accessory gene of human immunodeficiency virus type 1. FAESB Journal 13: 621–637.

Shimura M, Onozuka Y, Yamaguchi T, Hatake K, Takaku F, Ishizaka Y. 1999b. Micronuclei formation with chromosome breaks and gene amplification caused by Vpr, an accessory gene of human immunodeficiency virus type 1. Cancer Research 59: 2259–2264.

Singh NP, McCoy MT, Tice RR, Schneider EL. 1988. A simple technique for quantitation of low levels of DNA damage in individual cells. Experimental Cell Research 175: 184–191.

Skalka AM. Katz RA. 2005. Retroviral DNA integration and the DNA damage response. Cell Death and Differentiation 12: 971–978.

Stern M, Gonzalez Cid M, Larripa I, Slavutsky I. 1994. AZT-induction of micronuclei in human lymphocyte subpopulations. Toxicology Letters 70: 235–242.

Sun Y, Huang Y-C, Xu Q-Z, Wang H-P, Bai B, Sui J-L, Zhou P-K. 2006. HIV-1 Tat depresses DNA-PK_{CS} expression and DNA repair, and sensitises cells to ionising radiation. Int. J. Radiation Oncology Biol. Phys. 65: 842–850.

Thierens H, Vral A, De Ridder L. 1996. A cytogenetic study of radiological workers: effect of age, smoking and radiation burden on the micronucleus frequency. Mutation Research 360: 75–82.

Thierens H, Vral A, Barbe M, Aousalah B, De Ridder L. 1999. A cytogenetic study of nuclear power plant workers using the micronucleus-centromere assay. Mutation Research 445: 105–111.

Tubiana M, Dutreix J, Wambarsie A. 1990. Introduction to Radiobiology. London: Taylor and Francis.

Tucker JD. 2008. Low-dose ionizing radiation and chromosome translocations: A review of the major considerations for human biological dosimetry. Mutation Research/ Reviews in Mutation Research, 659: 211–220.

Varga D, Johannes T, Jainta S, Schuster S, Schwarz-Boeger U, Kiechle M, Patino Garcia B, Vogel W. 2004. An automated scoring procedure for the micronucleus test by image analysis. Mutagenesis 19: 391–397.

Vral A, Thierens H, De Ridder L. 1997. In vitro micronucleus-centromere assay to detect radiation-damage induced by low doses in human lymphocytes. Int.J. Radiat. Biol. 71: 61–68.

Weier HUG, Lucas JN, Poggensee M, Segraves R, Pinkel D, Gray JW. 1991. Two-color hybridisation with high complexity chromosome-specific probes and a degenerate alpha satellite probe DNA allows unambiguous discrimination between symmetrical and asymmetrical translocation. Chromosoma 100: 371–376.

Weng H, Morimoto K. 2009. Differential responses to mutagens among human lymphocyte subpopulations. Mutation Research 672: 1–9.

Wilkins RC, Wilkinson D, Maharaj HP, Bellier PV, Cybulski MB, McLean JRN. 2002. Differential apoptotic response to ionising radiation in subpopulations of human white blood cells. Mutation Research 513: 27–36.

Willems P, August L, Slabbert J, Romm H, Oestreicher U, Thierens H, Vral A. 2010. Automated micronucleus (MN) scoring for population triage in case of large scale radiation events. International Journal of Radiation Biology 86: 2–11.

Wojcik A, Kowalska M, Bouzyk E, Buraczewska I, Kobialko G, Jarocewicz N, Szumiel I. 2000. Validation of the micronucleus-centromere assay for biological dosimetry. Genetics and Molecular Biology 23: 1083–1085.

Wolff S. 1998. The Adaptive Response in Radiobiology: Evolving Insights and Implications. Environmental Health Perspectives 106: 277–283.

Wuttke K, Streffer C, Muller W-U. 1993. Radiation induced micronuclei in subpopulation of human lymphocytes. Mutation Research 286: 181–188.

Zielhuis RL. 1984. Recent and potential advances applicable to the protection of workers' health – biological monitoring. II. In: Berlin A, Yodaiken RE, Henman BA (Eds.), Assessment of toxic agents at the workplace – roles in ambient and biological monitoring. Martinus Nijhoff Publishers, Boston.

Appendix A

Product List

Cytogenetic tests:

Complete medium for method 1:	500 ml RPMI 1640 (Biowhittaker-Lonza), 75 ml Foetal Calf Serum, 5 ml penicillin/streptomycin (Gibco).
Complete medium for method 2:	500 ml RPMI 1640, 10 ml L-glutamine (Gibco), 2.4 ml penicillin/streptomycin.
Phytohaemagglutinin (Invitrogen)	
Cytochalasin B:	25 mg cytochalasin B (Sigma Aldrich) 3.3 ml DMSO (Sigma)
KCl (per 1l):	5.6 g KCl (Merck) dH_2O
Methanol (Merck)	
Acetic acid (Merck)	
Ringer (per 500ml):	4.5 g NaCl (AAR) 0.21 g KCl (Merck) 0.12 g $CaCl_2$ dH_2O

Slide Staining:

Acridine orange work solution: 0.4 ml stock
40 ml dH_2O

Acridine orange stock solution: 0.1 g acridine orange stain
100 ml dH_2O

Acridine orange buffer: 1 tablet
1 l dH_2O

Vectashield with DAPI (Vector Labs)

FISH:

Ethanol (Merck) 70 %, 90 %, 100 %

Pretreatments:

RNase (100 µg/ml RNase) (per 1 ml): 200 µl 500 µg/ml RNase (Roche)
800 µl 2 × SSC

1 × PBS: 137 mM NaCl
2.7 mM KCl
10 mMNa_2HPO_4
1.76 mM KH_2PO_4
dH_2O
pH = 7.4

Pepsin (3.5.1b): 0.5 µl of stock pepsin
1 ml 10 mM HCl

Stock pepsin (1 mg/ml)(Sigma)

HCl (10 mM) (10 ml)	1 ml 0.1 N HCl 9 ml dH_2O
Pepsin solution (3.5.1c):	0.001 % pepsin 0.01 M HCl
Postfixation buffer:	1 × PBS 0.05 M MgCl2
4 % paraformaldehyde:	4 % PFA 1 × PBS, 0.05 M MgCl2
1 N HCl (per 1 l):	31 ml 37 % hydrochloric acid (fuming) (Merck) 1 l dH_2O
0.1 N HCl (per 1 l):	100 ml 1 N HCl 900 ml dH_2O
Pepsin (3.5.1d):	25 mg pepsin (Sigma) 50 ml 01 N HCl

NB: The pepsin is only added when the 01 N HCl solution is at 37 °C, and the measurements need to be accurate.

1 % formaldehyde (per 500 ml)	13.5 ml 37 % formaldehyde dH_2O pH = 7 (with NaOH)

Hybridisation:

Denaturing solution (per 50 ml): 35 ml deionised formamide,
5 ml phosphate buffer,
5 ml 20 × SSC,
5 ml dH_2O
pH = 7 (HCl)

STARFISH© denaturing solution: 70 % formamide (deionised)
2 × SSC

Deionised formamide (per 1 l): 1 l formamide (Merck)
10 heaped scoops of analytical grade mixed bed resin (Biorad)

Stirred for 2 hours, and filtered with Whatman filter paper

Phosphate buffer (per 1 l): 413 ml solution A
587 ml solution B
pH = 7 (Solution A and B used to adjust pH)

Solution A (acid) (per 1 l): 9.08 g KH_2PO_4 (Saarchem)
dH_2O

Solution B (base) (per 1 l): 11.88 g $Na_2PO_4.2H_2O$ (Saarchem)
dH_2O

20×SSC (per 1 l): 175 g NaCl
88.23 g tri-sodium citrate
dH_2O
pH = 7 (HCl)

STARFISH© commercial pan-centromeric probe (Cambio)

Washing:

2 × SSC (per 150 ml):	15 ml 20 × SSC 135 ml dH_2O
2 × SSC/0.1 % Tween:	50 ml 2 × SSC 50 µl Tween 20 (Merck)
50 % formamide (per 150 ml):	15 ml 20 × SSC 65 ml dH_2O 70 ml formamide (Merck); not deionised
DAPI stock solution (0.2 mg/ml):	10 mg DAPI (Merck) 50 ml 2 × SSC
DAPI work solution:	50 µl DAPI stock 50 ml 2 × SSC
Vectashield (Vector labs)	
Rubber cement	Fixogum (Marabu)

Bacterial culture:

Luria Broth medium (per 500 ml):	5 g tryptone (Merck) 2.5 g yeast extract (Merck) 5 g NaCl dH_2O

Ampicillin 50 mg/ml:	0.5 g ampicillin 10 ml dH_2O

Plasmid extraction:

Qiagen Plasmid Midi Kit

Buffer P1:	50 mM Tris-Cl (pH = 8), 10 mM EDTA, 100 µg/ml RNase A
Buffer P2:	200 mM NaOH, 1 % SDS (w/v)
Buffer P3:	3 M potassium acetate (pH = 5.5)
Buffer QBT:	750 mM NaCl, 50 mM MOPS (pH = 7), 15 % isopropanol (v/v), 0.15 % Triton® X-100 (v/v)
Buffer QC:	1 M NaCl, 50 mM MOPS (pH = 7), 15 % isopropanol (v/v)
Buffer QF:	1.25 M NaCl, 50m M Tris-Cl (pH = 8.5), 15 % isopropanol (v/v)

Isopropanol (BDH)

TE Buffer (Promega):	10 mM Tris-Cl (pH = 8) , 1 mM EDTA

DNA extraction:

Red blood cell lysis buffer (Roche)

Proteinase-K lysis buffer:	50 mM Tris-HCl, 1 mM EDTA, 0.5 % Tween, dH_2O pH = 8.8
Tris (1 M) (per 500 ml):	60.6 g Tris (Merck) dH_2O pH = 8.5
EDTA (0.5 M) (per 1 l):	186.1 g disodium EDTA-2H (Boehringer-Mannheim) dH_2O pH = 8
Proteinase-K (10 mg/ml):	10 mg proteinase-K (Roche) 1 ml dH_2O

Prepared on the day of use.

Phenol (Sigma-aldrich)

Chloroform (Sigma-aldrich)

PCR:

Forward primer (100 μM) (Operon biotechnologies):

50 nmol lyophilised primer

648 μl dH_2O

Reverse primer (100 μM) (Operon biotechnologies):

50 nmol lyophilised primer

517 μl dH_2O

10 × NH_4 reaction buffer (Bioline)	160 nM $(NH_4)_2SO_4$
	670 mM Tris-HCl (pH = 8.8)
	0.1 % stabiliser
$MgCl_2$ (10 mM):	10 μl 50 mM $MgCl_2$ (Bioline)
	40 μl dH_2O

BIOTAQ DNA polymerase (5 U/l)

Storage buffer:	20 mM Tris-HCl (pH = 7.5)
	100 mM NaCl
	0.1 mM EDTA
	2 mM DTT
	50 % glycerol and stabilisers
dNTP mix (40 mM):	10 mM dATP
	10 mM dCTP
	10 mM dGTP
	10 mM dTTP

PCR purification:

High Pure PCR Product Purification Kit (Roche)

Binding Buffer:	3 M guanidine-thiocyanate, 10 mM Tris-HCl, 5 % ethanol (v/v), pH = 6.6
Wash Buffer:	20 mM NaCl, 2 mM Tris-HCl, 80 % ethanol, pH = 7.5
Elution Buffer:	10 mM Tris-HCl, pH = 8.5

BioSpin PCR amplicon purification kit (BioFlux)

Direct labelling:

Nick translation buffer:	0.5 M Tris 50 mM MgCl2 0.5 mg/ml BSA (Roche) dH_2O
MgCl2 (1 M) (per 100 ml):	20.331 g MgCl2 (Sigma-aldrich) dH_2O
β-mercaptoethanol (0.1 M) (per 15 ml):	0.1 ml β-mercaptoethanol (Sigma) dH_2O

Table 5: Reagent volumes for dNTP mix

REAGENT	VOLUME (µl) × 1
dATP (10 mM) (Promega)	1.5
dCTP (10 mM) (Promega)	1.5
dGTP (10 mM) (Promega)	1.5
dTTP (10 mM) (Promega)	0.75
Spectrum Orange dUTP (1 mM) (Enzo)	7.5
dH_2O	17.25
TOTAL	30

dNTPs (10 mM): 10 µl 100 mM dNTP stock
90 µl dH_2O

Spectrum Orange dUTP (1 mM) (Enzo): 50 nmol lyophilised pellet
50 µl dH_2O

Hybridisation buffer: 50 % deionised formamide,
2 × SSC
10 % dextran sulphate (Sigma),
50 mM sodium dihydrogen orthophosphate
pH = 7

NaCl (0.3 M) (per 25 ml): 0.4383 g NaCl
dH_2O

10 % SDS (per 100 ml): 10 g SDS (BDH)
dH_2O

$NaAc_3$ (3 M) (per 100 ml): 24.609 g $NaAc_3$ (BDH)
dH_2O

DNase I stock solution:	3 mg DNase I (Roche)
	0.5 ml 0.3 M NaCl
	0.5 ml glycerol
DNase I work solution:	1 ml ice-cold dH_2O
	µl as required DNase I stock solution

Herring sperm DNA (10 mg/ml) (Promega)

Storage solution:	10 mM Tris-HCl (pH = 7.5)
	10 mM NaCl
	1 mM EDTA

Gel electrophoresis:

2 % agarose gels	0.8 g agarose (Bioline)
	40 ml 1 × TAE buffer / 0.5 × TBE buffer
	0.4 µl ethidium bromide

Instead of adding the ethidium bromide directly to the gel before electrophoresis, the gel could be immersed in an ethidium bromide bath after electrophoresis for 30 minutes.

50 × TAE buffer (1 l)	242 g Tris
	100 ml 0.5 M EDTA (pH = 8)
	57.1 ml glacial acetic acid
	dH_2O
1 × TAE buffer (1 l)	20ml 50 × TAE buffer
	dH_2O

10 × TBE buffer (1 l)	108 g Tris
	55 g boric acid
	40 ml 0.5 M EDTA (pH = 8)
	dH_2O
0.5 × TBE buffer (1 l)	50 ml 10 × TBE buffer
	dH_2O

6 × orange loading dye (Fermentas)

O'Gene Ruler 100 bp ladder (Fermentas)

Appendix B

A successful plasmid extraction is shown in Figure 16. The extracted DNA is electrophoresed on a 2 % agarose gel alongside λ DNA to determine if the extraction was successful, and to determine the concentration of the extracted DNA. A spectrophotometer could not be used as the genomic DNA would obstruct any reading.

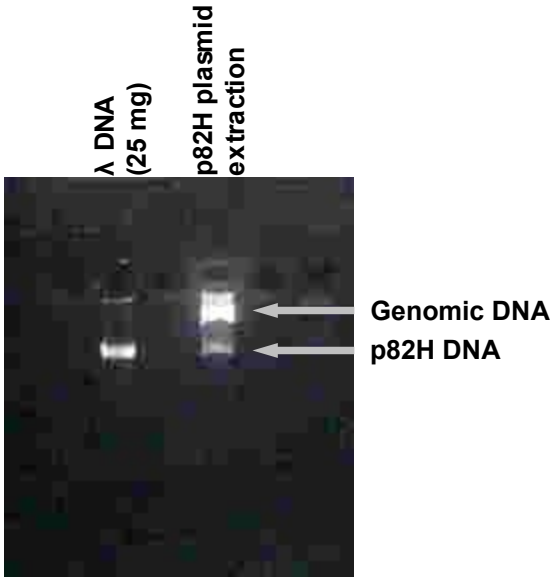

Figure 16: Extracted p82H DNA alongside lambda DNA

The p82H plasmid was directly labelled by means of nick translation, and it was deemed successful by gel electrophoresis as shown in Figure 17. A DNA smear between 200 bp and 500 bp should be visible, as well as incorporation of Spectrum Orange. Unincorporated Spectrum Orange dUTPs can be seen below the smear.

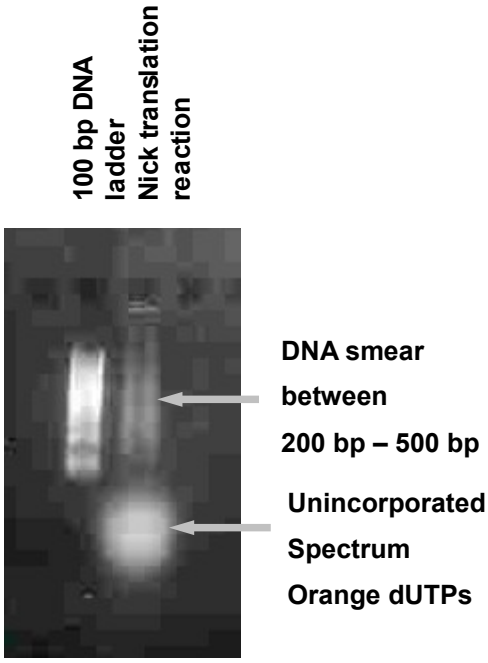

Figure 17: Direct labelling of extracted p82H DNA

PCRs were performed as stated in the methods, and were electrophoresed on a 2 % agarose gel (Figure 18). If two bands (at 175 bp and 345 bp) were visible, the reactions were regarded as successful (Weier et al, 1991). These PCRs were kept at 4 °C until they were purified with PCR purification kits (see Methods).

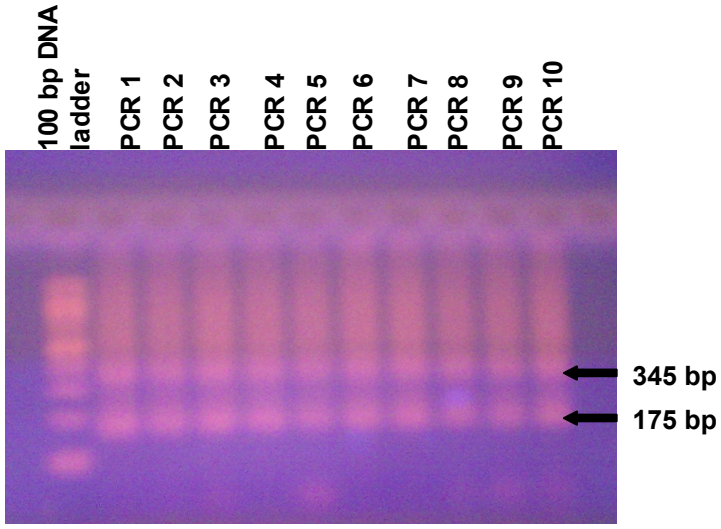

Figure 18: Successful PCR reactions (1–10) with two bands at 175 bp and 345 bp

Purified PCRs were directly labelled by means of nick translation (see Methods). The nick translation reaction underwent gel electrophoresis Figure 19. Similarly with the direct labelling of p82H, the reaction was seen as successful if a smear was seen between 200 bp and 500 bp.

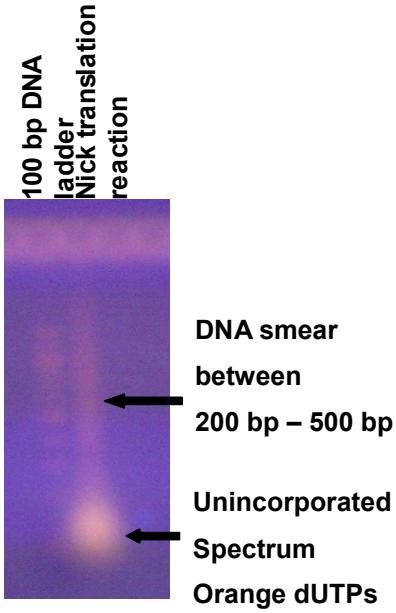

Figure 19: Direct labelling of purified PCR reaction